Sensor and Simulation Notes

Note 118

October 1970

Effect of Replacing One Conducting Plate of a Parallel-Plate
Transmission Line by a Grid of Rods

Lennart Marin
Northrop Corporate Laboratories
Pasadena, California

Abstract

The charge distribution is calculated on a grid of rods replacing one
of the conducting plates in a parallel-plate transmission line. Two cases
are investigated, namely, (1) a transmission line made up of a grid of rods
above one plate and (2) a transmission line made up of a grid of rods between
two plates. In each case numerical calculations are carried out for (1) the
maximum value of the normal component of the electric field at the surface
of each rod and (2) the effective electric height of the transmission line,
i.e., the height of a parallel-plate line having the same characteristic
impedance as the transmission line considered. The special case where the
grid of rods and the plate (or plates) are very far apart is treated in an
appendix.

Sensor and Simulation Notes

Note 118

October 1970


Effect of Replacing One Conducting Plate of a Parallel-Plate
Transmission Line by a Grid of Rods

Lennart Marin
Northrop Corporate Laboratories
Pasadena, California

## Abstract

The charge distribution is calculated on a grid of rods replacing one
of the conducting plates in a parallel-plate transmission line. Two cases
are investigated, namely, (1) a transmission line made up of a grid of rods
above one plate and (2) a transmission line made up of a grid of rods between
two plates. In each case numerical calculations are carried out for (1) the
maximum value of the normal component of the electric field at the surface
of each rod and (2) the effective electric height of the transmission line,
i.e., the height of a parallel-plate line having the same characteristic
impedance as the transmission line considered. The special case where the
grid of rods and the plate (or plates) are very far apart is treated in an
appendix.

# I. Introduction

A common type of EMP simulator is the parallel plate transmission line. In certain types of this transmission line one of the plates is replaced by a grid of rods parallel to the direction in which the electromagnetic pulse propagates. Then the question naturally arises concerning the field in the vicinity of the rods. As the radius of the rods gets smaller the normal component of the electric field at the surface of the rods becomes larger. Moreover, by replacing one of the plates in a parallel-plate transmission line by a grid of rods we increase the effective electric height of the transmission line. The purpose of this note is to work out in detail the maximum electric field at the surface of each rod and the effective electric height for two different situations: (1) a grid of rods above one plate and (2) a grid of rods between two plates.

The effect of replacing one conducting plate with a grid of rods has been considered in reference 1 where the rods are taken to be thin wires. Hence, the problems treated in reference 1 are just some limiting cases of this note.

The model chosen for study in section II is that of an infinite row of perfectly conducting cylinders above a perfectly conducting plane (see figure 1). This structure can sustain a TEM wave propagating parallel to the direction of the axis of the cylinders. It is well known that the problem of determining the transverse electric and magnetic fields of a TEM wave can be reduced to a two-dimensional electrostatic problem (see figure 3). We wish to calculate the fields in the neighborhood of each cylinder. This is done by first calculating the surface charge density on each cylinder. The normal component of the electric field at the surface of each cylinder is proportional to the charge density. Furthermore, the tangential magnetic field and hence the longitudial surface current for the TEM wave is proportional to this surface charge density. With knowledge of the charge density the fields anywhere can be calculated by computing a simple sum. Moreover, the admittance of the transmission line and hence the effective electric height of the line can be easily determined from the charge density.

In section III, we solve the problem of an infinite row of perfectly conducting cylinders between two perfectly conducting planes (see figure 2).

2

Assume that down this structure a TEM wave is propagating in which the electric field has equal magnitude but opposite direction on the two different sides of the grid. Again, we will solve this problem by reducing it to a two-dimensional electrostatic problem (see figure 4).

The numerical methods that are used to solve the two-dimensional electrostatic problems treated in sections II and III are presented in section IV. Graphs of the maximum value of the normal component of the electric field at the surface of each cylinder and the effective electric height of the lines are also presented in section IV.

In appendix A we derive some different expressions of the potential due to a lattice of line charges. The special case when the grid of rods and the perfectly conducting plane or planes are very far apart is treated separately in appendix B.

## II.  A Grid of Rods Above One Plate

In this section we will determine the electric field of a TEM wave on the waveguide shown in figure 1 by solving the following electrostatic problem. Consider an infinite row of parallel perfectly conducting cylinders above a perfectly conducting plane as shown in figure 3.  The radius of each cylinder is a and the spacing between the centers of two neighboring cylinders is 2d. The centers of all cylinders lie in a common plane parallel to and at the distance h from the perfectly conducting plane (see figure 3).  Moreover, suppose that the potential on each cylinder is $V_o$ and that the potential on the perfectly conducting plane is 0.

In the region $y > - h$, the influence on the field due to the perfectly conducting plane $y = - h$ can be taken into account by replacing it by an infinite row of image cylinders all having the potential $- V_o$ (see figure 3).[*] From the symmetry of the problem it follows that we can make the following Fourier series expansion of the charge distribution, $\sigma_k(\theta_k)$, on the cylinder with center at $x = 2kd$  $(k = \ldots -2, -1, 0, 1, 2, \ldots)$ and $y = 0$

$$\sigma_k(\theta_k) = \sigma_o(\theta_k) = \sum_{n=0}^{\infty} s_n \cos n\theta_k \quad . \tag{1}$$

The charge distribution, $\sigma_k'(\phi_k)$, on the image cylinder with center at $x = 2kd$ and $y = - 2h$ is then given by

$$\sigma_k'(\phi_k) = - \sigma_o(\pi - \phi_k) = - \sum_{n=0}^{\infty} (-1)^n s_n \cos n\phi_k \quad . \tag{2}$$

In the region $y > - h$ but outside the primary cylinders we have the potential

$$\phi_e(x,y) = f_e(x,y) + \sum_{n=1}^{\infty} \sum_{k=-\infty}^{\infty} \frac{a s_n}{2n\varepsilon_o} \left[ \left(\frac{a}{r_k}\right)^n \cos n\theta_k - \left(\frac{-a}{\rho_k}\right)^n \cos n\phi_k \right] \tag{3}$$

where $r_k$, $\rho_k$, $\theta_k$ and $\phi_k$ are defined in figure 3.  The function $f_e(x,y)$ is the potential due to the net charges on the primary and image cylinders, i.e., the potential due to two sets of line charges.  The potential from these line charges may be accounted for by solving with the aid of conformal mapping the

---

[*] Thus, the original problem is transformed to the electrostatic problem of two parallel grids of rods having the potentials $V_o$ and $-V_o$, respectively.

electrostatic problem of one set of line charges above a perfectly conducting plane. Thus,

$$f_e(x,y) = \frac{as_o}{2\epsilon_o} \ln\{\frac{\cosh[\pi(y+2h)/d] - \cos(\pi x/d)}{\cosh(\pi y/d) - \cos(\pi x/d)}\}$$

Inside one of the primary cylinders, e.g. the 0-th cylinder, we have the potential

$$\phi_i(x,y) = f_i(x,y) + \sum_{n=1}^{\infty} \sum_{k=-\infty}^{\infty}{}' \frac{as_n}{2n\epsilon_o} [(\frac{a}{r_k})^n \cos n\theta_k - (\frac{-a}{\rho_k})^n \cos n\phi_k]$$

$$+ \sum_{n=1}^{\infty} \frac{as_n}{2n\epsilon_o} [(\frac{r_o}{a})^n \cos n\theta_o - (\frac{-a}{\rho_o})^n \cos n\phi_o] \qquad (4)$$

where

$$f_i(x,y) = \frac{as_o}{2\epsilon_o} \ln\{\frac{\cosh[\pi(y+2h)/d] - \cos(\pi x/d)}{\cosh(\pi y/d) - \cos(\pi x/d)} \cdot \frac{x^2+y^2}{a^2}\}$$

and the prime on the summation indicates the ommision of the k = 0 term.

Within the perfectly conducting cylinders the potential is constant. This condition can be ensured by putting $\phi_i(0,0) = V_o$ and all the partial y-derivatives of $\phi_i(x,y)$ equal to zero at the origin. As mentioned in reference 2, another procedure leading to the same condition on $s_n$ is to expand $\phi_e(x,y)$ on the surface of one primary cylinder in a Fourier cosine series and to equate all Fourier constants in this expansion to zero except the first. Both methods lead to the following system of equations

$$\frac{\epsilon_o V_o}{a} = \frac{s_o}{2} \ln\{\frac{2d^2}{\pi^2 a^2} [\cosh(\frac{2\pi h}{d}) - 1]\}$$

$$+ \sum_{n=1}^{\infty} \frac{s_n}{n} \{\sum_{k=1}^{\infty} [(\frac{a}{2kd})^n \cos \frac{n\pi}{2} - (\frac{-a}{b_k})^n \cos n\beta_k] - \frac{1}{2} (\frac{-a}{2h})^n\} \qquad (5a)$$

5

$$0 = s_o \left\{ - \frac{(-1)^\ell (\ell-1)!}{(2h)^\ell} + \sum_{k=1}^{\infty} \left[ \frac{(-1)^\ell 2(\ell-1)! \cos \ell\pi/2}{(2kd)^\ell} - \frac{(-1)^\ell 2(\ell-1)! \cos \ell\beta_k}{b_k^\ell} \right] \right.$$

$$+ \sum_{n=1}^{\infty} \frac{s_n}{n} \left\{ \frac{\ell!}{2a^\ell} \delta_{n\ell} - \frac{(-1)^\ell (\ell+n-1)! (-a)^n}{2(n-1)! (2h)^{\ell+n}} \right.$$

$$+ \sum_{k=1}^{\infty} \left[ \frac{(-1)^\ell (\ell+n-1)! a^n \cos[(\ell+n)\pi/2]}{(n-1)! (2kd)^{\ell+n}} \right.$$

$$\left. \left. - \frac{(-1)^\ell (\ell+n-1)! (-a)^n \cos[(\ell+n)\phi_k]}{(n-1)! \, b_k^{n+\ell}} \right] \right\} \quad , \qquad \ell \geq 1 \tag{5b}$$

where

$$\beta_k = \tan^{-1}(kd/h)$$

and

$$b_k = 2\sqrt{h^2 + k^2 d^2} \qquad .$$

This system of equations can be simplified to

$$\sum_{n=0}^{\infty} N_{\ell n} x_n = \delta_{\ell o} \qquad . \tag{6}$$

Here,

$$x_n = \pi a h s_n / (d\varepsilon_o V_o) \quad ,$$

$$N_{oo} = \frac{1}{2} \alpha\pi^{-1} \ln\{2\alpha^2 [\cosh(2\pi/\alpha) - 1]/(\pi^2\beta^2)\}$$

$$N_{on} = \alpha/(\pi n)[A_n(\alpha,\beta) - C_n(\alpha,\beta) - \frac{1}{2}(-\beta/2)^n] \quad , \quad n \geq 1 \quad ,$$

$$N_{\ell o} = 4[(-1)^\ell A_\ell(\alpha,\beta) - C_\ell(\alpha,\beta) - \frac{1}{2}(-\beta/2)^\ell] \quad , \quad \ell \geq 1 \quad ,$$

$$N_{\ell n} = \delta_{\ell n} + 2\binom{\ell+n-1}{n}\left[(-1)^{\ell}A_{\ell+n}(\alpha,\beta) - C_{\ell+n}(\alpha,\beta)\right.$$

$$\left. - \frac{1}{2}(-\beta/2)^{\ell+n}\right] \quad , \quad \ell \geq 1 \quad , \quad n \geq 1 \quad ,$$

$$\alpha = d/h$$

$$\beta = a/h$$

$$C_q(\alpha,\beta) = (-\beta/2)^q \sum_{k=1}^{\infty} \frac{\cos(q\beta_k)}{(1+\alpha^2 k^2)^{q/2}}$$

$$= (-\beta/2)^{q+1}\left\{\frac{\pi}{\beta(q-1)!}\left[\frac{d^{q-1}}{dz^{q-1}}(\coth \pi z)\right]_{z=-\alpha^{-1}} + \beta^{-1}\right\}$$

$$A_q(\alpha,\beta) = \begin{cases} 0 \quad , & q \text{ odd} \\ (-1)^{q/2}(\tfrac{1}{2}\beta/\alpha)^q \zeta(2q) = \frac{1}{2}(-1)^{q/2}\pi^q B_{q/2}(\beta/\alpha)^q/q! \quad , & q \text{ even} \end{cases}$$

where $\zeta(x)$ is the Riemann zeta function and the $B_n$'s are the Bernoulli numbers.

After having solved the system of equations (6) the field outside the primary cylinders and above the perfectly conducting plane can be evaluated from the gradient of equation (4).

A quantity of interest here is the admittance of the transmission line or, equivalently, the capacitance per unit cell, C, between the grid of cylinders and the perfectly conducting plane. In this connection we introduce the effective electric height, $h_1$, of the transmission line, i.e., the height of a parallel plate transmission line having the same admittance as the transmission line considered in this section (see figure 5). The quantities C and $h_1$ are given by

$$C = 2\pi a s_o/V_o = 2d\varepsilon_o x_o/h \tag{7}$$

7

and

$$h_1 = V_o \varepsilon_o d/(\pi a s_o) = h/x_o \quad . \tag{8}$$

The incremental effective electric height, $\Delta h$, of the structure is given by

$$\Delta h = h_1 - h = h(x_o^{-1} - 1) \quad . \tag{9}$$

For $d \ll h$ and $a \ll d$ we can solve the system of equations (6) approximately by perturbation methods and get

$$x_o \approx 1 - d\pi^{-1}h^{-1} \ln(d\pi^{-1}a^{-1}) \quad .$$

Thus,

$$\Delta h \approx d\pi^{-1} \ln(d\pi^{-1}a^{-1}) \tag{10}$$

and this expression for $\Delta h$ coincides with the expression given by equation (88) in reference 1. The case when $d \gg h$ can be studied with the aid of the solution of the electrostatic problem of two coupled cylinders[3]. This study leads to the following approximate expression

$$\Delta h \approx d\pi^{-1} \ln[(h + \sqrt{h^2 - a^2})/a] - h \quad . \tag{11}$$

The normal component, $E_n(\theta_k)$, of the electric field at the surface of one of the cylinders is given by

$$E_n(\theta_k) = \varepsilon_o^{-1}\sigma_o(\theta_k) = \varepsilon_o^{-1} \sum_{n=1}^{\infty} s_n \cos n\theta_k \quad . \tag{12}$$

The relative field distribution, $e(\theta_k)$, (field enhancement factor) is defined as the normal component of the electric field at each rod divided by the mean value of the normal component of the electric field at the perfectly conducting plane. Thus, we have

$$e(\theta_k) = d\sigma_o(\theta_k)/(\pi a s_o) = d(\pi a x_o)^{-1} \sum_{n=0}^{\infty} x_n \cos n\theta_k \tag{13}$$

8

and

$$e_1 = \max_{\theta_k}\{e(\theta_k)\} = e(\pi) = d(\pi a x_o)^{-1} \sum_{n=0}^{\infty} (-1)^n x_n \tag{14}$$

For $d \ll h$ and $a \ll d$ we have approximately

$$e_1 \approx d\pi^{-1}a^{-1} \tag{15}$$

and this expression for $e_1$ can be obtained by taking the proper limit of equation (92) in reference 1. For $d \gg h$ we have

$$e_1 \approx d\pi^{-1}(a - h + \sqrt{h^2 - a^2})^{-1} \quad . \tag{16}$$

The quantities $e_1$ and $\eta$,

$$\eta = \Delta h/h \quad , \tag{17}$$

are graphed in figures 7-16 for a wide range of $d/h$ and $a/h$.

9

### III.  A Grid of Rods Between Two Plates

In this section, we will determine the electric field of a TEM wave on the waveguide shown in figure 2 by solving the following electrostatic problem.  Consider an infinite row of perfectly conducting cylinders between two parallel perfectly conducting planes.  The radius of each cylinder is a and the spacing between the centers of two neighboring cylinders is 2d.  The centers of all cylinders lie in a common plane parallel to and at the distance $D/2 + y_o$ from one of the perfectly conducting planes.  Here D is the distance between the two perfectly conducting planes and $0 \leq |y_o| < D/2 - a$ (see figure 4).  Moreover, suppose that the potential on each cylinder is $V_o$ and that the potential on the two perfectly conducting planes is 0.

By the method of images the potential between the two plates can be determined from the two dimensional lattice shown in figure 4.  From the symmetry of the problem it follows that we can make the following Fourier series expansion of the charge distribution, $\sigma_{mk}(\theta_{mk})$, on the cylinder with center at $x = 2kd$ (k = ..., -2, -1, 0, 1, 2, ...) and $y = mD - [1 - (-1)^m]y_o$ (m = ..., -2, -1, 0, 1, 2, ...),

$$\sigma_{mk}(\theta_{mk}) = \begin{cases} \sigma_o(\theta_{mk}) = \sum_{n=0}^{\infty} s_n \cos \theta_{mk} \, , & m \text{ even} \\[3mm] - \sigma_o(\pi - \theta_{mk}) = - \sum_{n=0}^{\infty} (-1)^n s_n \cos \theta_{mk} \, , & m \text{ odd} \end{cases} \qquad (18)$$

Here $\sigma_o(\theta_{ok})$ is the charge distribution on one of the primary cylinders, and the angle $\theta_{mk}$ is defined in figure 4.  Following the procedure in section II the potential, $\phi_e(x,y)$, between the plates but outside the cylinders and the potential, $\phi_i(x,y)$, inside the primary cylinders are

$$\phi_e(x,y) = g_e(x,y) + \sum_{n=1}^{\infty} \frac{as_n}{2\varepsilon_o n} \sum_{m,k} \varepsilon_{mn} (\frac{a}{\rho_{mk}})^n \cos n\theta_{mk} \qquad (19)$$

$$\phi_i(x,y) = g_i(x,y) + \sum_{n=1}^{\infty} \frac{as_n}{2\varepsilon_o n} (\frac{\rho_{oo}}{a})^n \cos n\theta_{oo}$$

$$+ \sum_{n=1}^{\infty} \frac{as_n}{2\varepsilon_o n} \sum_{m,k}' \varepsilon_{mn} (\frac{a}{\rho_{mk}})^n \cos n\theta_{mk} \qquad (20)$$

10

where

$$\varepsilon_{mn} = \begin{cases} 1 \quad , & m \text{ even} \\ \\ -(-1)^n \quad , & m \text{ odd} \end{cases} \quad ,$$

the distance $\rho_{mk}$ is defined in figure 4 and the prime indicates omission of the term $m = k = 0$ in the summation where $-\infty < m < \infty$ and $-\infty < k < \infty$. The functions $g_e(x,y)$ and $g_i(x,y)$ are the potentials due to the net charges on the cylinders and their respective expressions are derived in appendix A.

Using the fact that inside each cylinder the potential is constant and hence all its derivatives are zero we arrive at the following system of equations

$$V_o = g_i(0,0) + \sum_{n=1}^{\infty} \frac{as_n}{2n\varepsilon_o} \sum_{m,k}' \varepsilon_{mn} \left(\frac{a}{b_{mk}}\right)^n \cos n\beta_{mk}$$

$$0 = s_o \sum_{m,k}' \frac{(-1)^m (\ell-1)! \, \cos(\ell\beta_{mk})}{b_{mk}^{\ell}} \tag{21}$$

$$+ \sum_{n=1}^{\infty} \frac{s_n}{2n} \left\{ \frac{\ell!}{a^{\ell}} \delta_{\ell n} + \sum_{m,k}' \frac{\varepsilon_{nm} (\ell+n-1)! a^n \cos[(\ell+n)\beta_{mk}]}{(n-1)! \, b_{mk}^{\ell+n}} \right\}$$

where

$$b_{mk} = \sqrt{(mD - d_m)^2 + 4k^2 d^2} \quad ,$$

$$d_m = [1 - (-1)^m] y_o$$

and

$$\beta_{mk} = \begin{cases} \tan^{-1}[2kd/(mD - d_m)] \quad , & m \neq 0 \\ \\ -\frac{\pi}{2} \operatorname{sgn}(k) \quad , & m = 0 \end{cases} \quad .$$

Suppose, here and after that $y_o = 0$, that is to say, the rods are situated symmetrically with respect to the two plates. From the symmetry of the problem

it then follows that $s_n = 0$ for $n$ odd. The original system of equations (21) can then be reduced to

$$\sum_{n=0}^{\infty} K_{\ell n} x_n = \delta_{\ell o} \qquad (22)$$

where

$$x_n = \pi a D/(4\varepsilon_o V_o d) s_{2n}$$

$$K_{oo} = (4\gamma/\pi)\left[\ln(2\pi^{-1}\xi^{-1}) - 2\sum_{k=1}^{\infty} \ln \tanh(\pi\gamma k)\right]$$

$$= 1 + (4\gamma/\pi)\ln(\gamma\pi^{-1}\xi^{-1}) - (8\gamma/\pi)\sum_{k=1}^{\infty} (-1)^k \ln(1 - e^{-\pi k/\gamma})$$

$$K_{on} = \gamma\pi^{-1}n^{-1}F_n(\gamma,\xi) \quad , \qquad\qquad n \geq 1$$

$$K_{\ell o} = 2F_\ell(\gamma,\xi) \quad , \qquad\qquad \ell \geq 1$$

$$K_{\ell n} = \delta_{\ell n} + \binom{2\ell+2n-1}{2n}F_{\ell+n}(\gamma,\xi) \quad , \qquad \ell \geq 1 \quad , \quad n \geq 1$$

$$\gamma = d/D$$

$$\xi = a/D$$

$$F_q(\gamma,\xi) = \xi^{2q}\sum_{m,k}' \frac{(-1)^m \cos(2q\beta_{mk})}{(m^2+4\gamma^2 k^2)^q} = \xi^{2q}\sum_{m,k}' (-1)^m (m + i2\gamma k)^{-2q} \quad .$$

Making use of the theory of elliptic functions we have

$$F_1(\gamma,\xi) = -\xi^2 P(1;1,i\gamma)$$

$$F_q(\gamma,\xi) = \xi^{2q}[c_q/(2q-1) - P^{(2q-2)}(1;1,i\gamma)/(2q-1)!] \quad , \quad q \geq 2 \tag{23}$$

where $P(x;\omega_1,\omega_2)$ is the Weierstrass elliptic function,

$$c_q = 3(2q+1)^{-1}(q-3)^{-1}\sum_{m=2}^{q-2} c_m c_{q-2} \quad , \quad q \geq 4 \quad ,$$

$$c_2 = g_2/20 \quad , \quad c_3 = g_3/28$$

and

$$g_2 = g_2(1,i\gamma) \quad , \quad g_3 = g_3(1,i\gamma)$$

are the invariants of the Weierstrass elliptic function.

The admittance, Y, of the transmission line for the symmetric TEM wave is determined by the capacitance, C, per unit cell between the grid of cylinders and the two perfectly conducting planes. The capacitance is given by

$$C = 2\pi a s_0/V_0 = 8d\epsilon_0 x_0/D \quad . \tag{24}$$

In this connection, we define an effective height, $D_1$, of the transmission line, i.e., the height of a three-plate transmission line having the admittance Y (see figure 6). Equating (24) to the capacitance of the three-plate line per 2d, we have

$$D_1 = D/x_0 \tag{25}$$

Define $\Delta$ to be

$$\Delta = \frac{1}{2}(D_1 - D) = \frac{1}{2}D(x_0^{-1} - 1) \quad . \tag{26}$$

13

For d << D and a << d we can solve the system of equations (22) by perturbation methods and get

$$\Delta \approx 2d\pi^{-1} \ln(d\pi^{-1}a^{-1}) \quad . \tag{27}$$

This expression for $\Delta$ coincides with the expression given by equation (100) in reference 1. For d >> h we can neglect the interaction between the primary cylinders and get the approximate expression

$$\Delta \approx 4d\varepsilon_o C_1^{-1} - \frac{1}{2} D \tag{28}$$

where $C_1^{-1}$ is the capacitance between one cylinder and two parallel plates. When D - 2a << D we can determine $C_1$ approximately by studying the problem of two coupled cylinders[3]. This study leads to the following approximate expression

$$\Delta \approx d\pi^{-1} \ln[(D + \sqrt{D^2 - 4a^2})/2a] - \frac{1}{2} D \quad . \tag{29}$$

The normal component, $E_n(\theta_k)$, of the electric field at the surface of one of the cylinders is given by

$$E_n(\theta_{ok}) = \varepsilon_o^{-1}\sigma_o(\theta_{ok}) = \varepsilon_o^{-1} \sum_{n=0}^{\infty} s_{2n} \cos(2n\theta_{ok}) \quad . \tag{30}$$

The relative field distribution, $e(\theta_{ok})$, (field enhancement factor) is

$$e(\theta_{ok}) = 2d\sigma_o(\theta_{ok})/(\pi a s_o) = 2d(\pi a x_o)^{-1} \sum_{n=0}^{\infty} x_n \cos(2n\theta_{ok}) \tag{31}$$

and define

$$e_2 = \max_{\theta_{ok}}\{e(\theta_{ok})\} = 2d(\pi a x_o)^{-1} \sum_{n=0}^{\infty} x_n = 2\gamma(\pi\xi x_o)^{-1} \sum_{n=0}^{\infty} x_n \quad . \tag{32}$$

For d << h and a << d we have approximately

$$e_2 \approx 2d\pi^{-1}a^{-1} \tag{33}$$

14

and this expression for $e_2$ can be obtained by taking the proper limit of equation (104) in reference 1. For $d \gg h$ and $D - 2a \ll D$ we have

$$e_2 \approx 2d\pi^{-1}/(2a - D + \sqrt{D^2 - 4a^2}) \quad . \tag{34}$$

The quantities $e_2$ and $\delta$,

$$\delta = \Delta/D \quad , \tag{35}$$

are graphed in figures 17-25 for a wide range of $d/D$ and $a/D$.

## IV. Numerical Results

The systems of equations (6) and (22) were solved numerically by keeping only ten equations and ten unknowns. Then, twenty unknowns and twenty equations were taken and solved numerically. The difference in the charge density computed from these two solutions was so small for all cases studied here that the numerical data from the twenty-by-twenty solution can be considered accurate to four digits.

Figures 7-10 show the normalized incremental effective height, $\eta$, of the transmission line treated in section II. In figure 7 we have also for $\beta = .05, .03, .01$ and $\beta \leq \alpha \leq .10$ graphed the approximative expression for $\eta$ that can be obtained from equation (10). For $\beta \leq .004$ and $.01 < \alpha < .1$ the difference between the expressions (9) and (10) for $\eta$ is negligable. Figure 11 shows the limiting value of $\Delta h/d$ as h tends to infinity. The broken curve represents the approximate value of $\Delta h/d$ given by (10).

Figures 12-15 show the function $e_1$ defined by equation (14) in section II. While figures 12-14 is a graph of $e_1$ as a function of $\alpha$ with $\beta$ as a parameter figure 15 is a graph of $e_1$ as a function of $\beta$ with $\alpha$ as a parameter. In figure 12 we have also graphed the approximate expression (15) for $e_1$. For $\beta \leq 10^{-3}$ and $\alpha > 10^{-2}$ the difference between (14) and (15) is negligable. In figure 14 we have added a graph of the approximate expression (16) for $e_1$. For $\beta < .2$ and $\alpha > 2$ the difference between (14) and (16) is negligable. Figure 16 shows the limiting value of $e_1$ as h tends to infinity. The broken curve represents the approximate value of $e_1$ given by (15).

Figures 17-19 show the normalized difference, $\delta$, between the effective electric height and the actual height of the transmission line treated in section III. In figure 17 we have for $\xi = .06, .04, .02$ and $\xi \leq \gamma \leq .11$ included a graph of the approximate expressions for $\delta$ that can be obtained from equation (27). For $\xi \leq .01$ and $.01 \leq \gamma \leq .1$ the difference between (26) and (27) is negligable. Figure 20 shows the limiting value of $\Delta/d$ as D tends to infinity. The broken curve represents the approximate value of $e_2$ given by (27).

Figures 21-24 show the normalized value, $e_2$, of the maximum electric field at the surface of the rods. In figure 18 we have also graphed the

16

approximate expression (33) for $e_2$. For $\xi < 2 \cdot 10^{-3}$ and $\gamma > 10^{-2}$ the difference between (32) and (33) is negligable. Figure 25 shows the limiting value of $e_2$ as D tends to infinity. The broken curve represents the approximate value of $e_2$ given by (33).
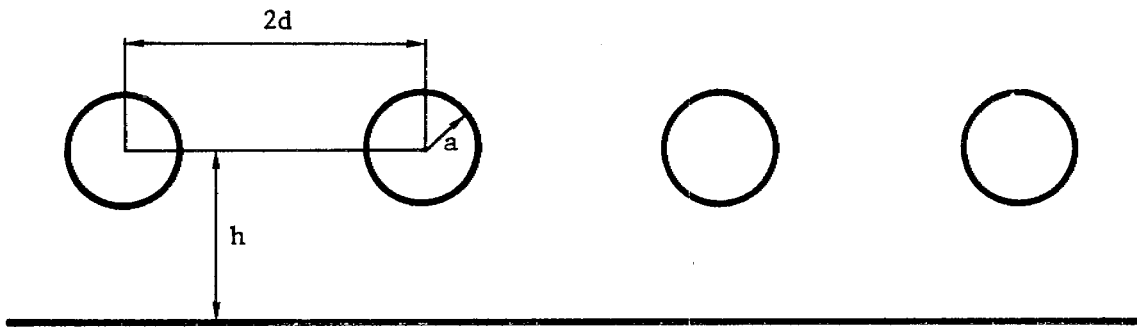
Figure 1.  Cross-section of transmission line consisting of one plate and a grid of rods.
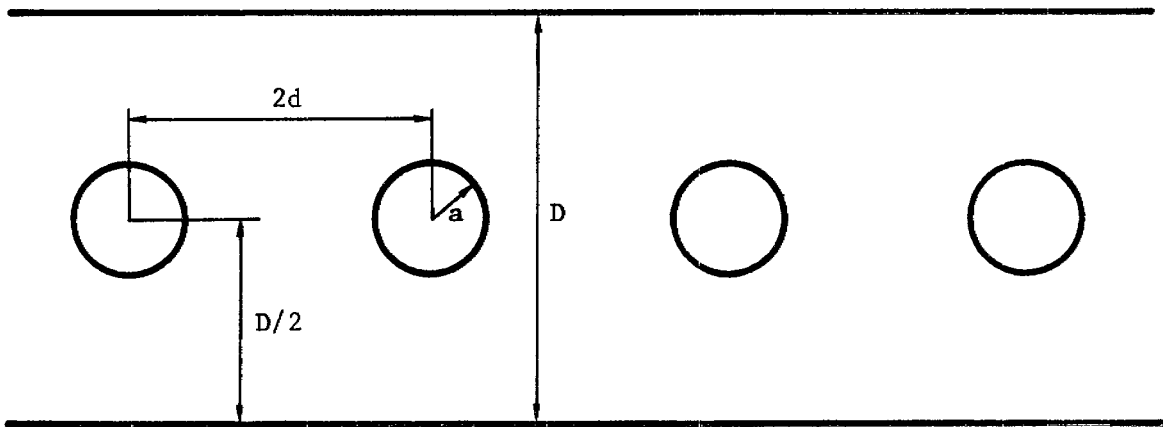


Figure 2.  Cross-section of transmission line consisting of two plates and a grid of rods.
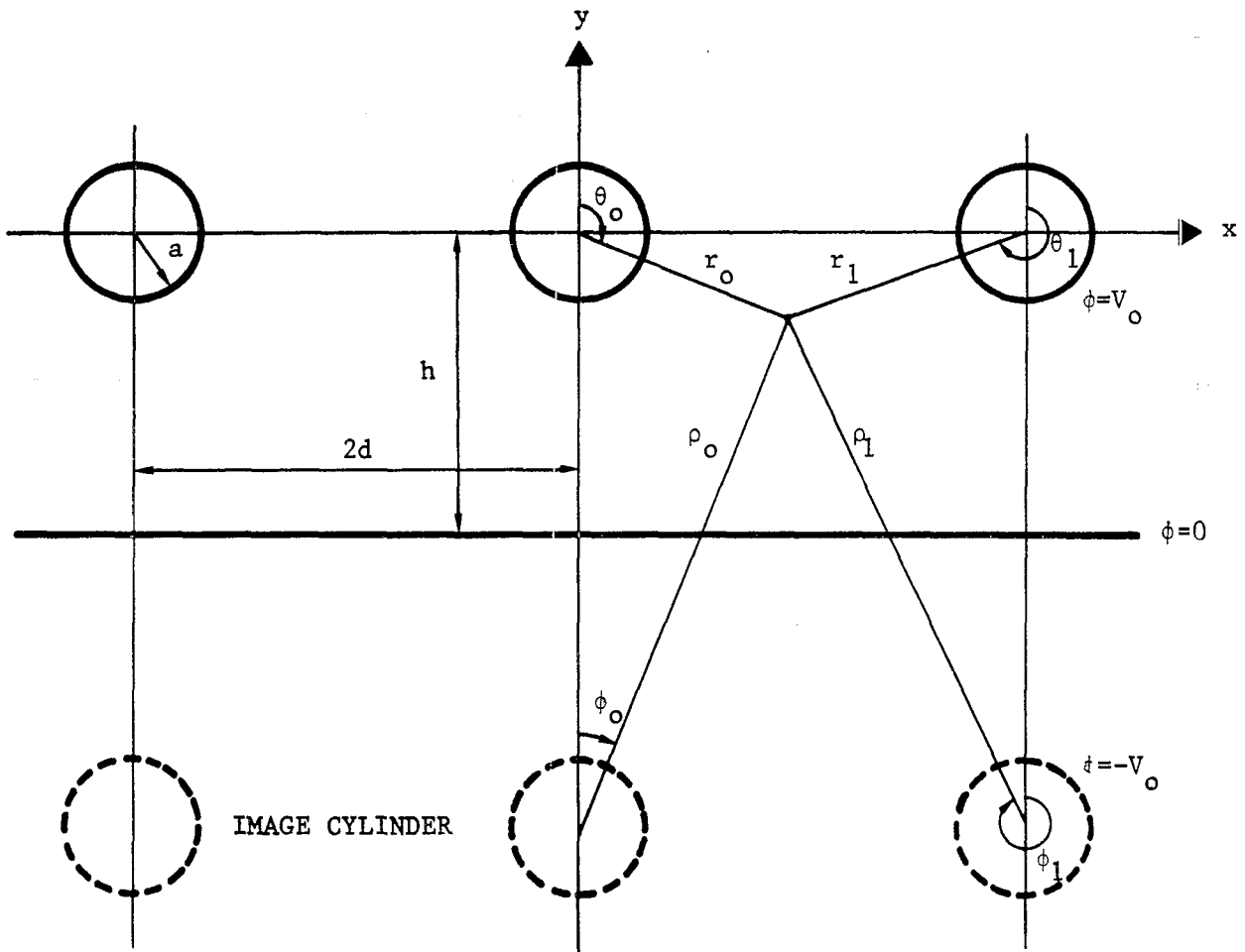
Figure 3. Two-dimensional electrostatic problem treated in section II.
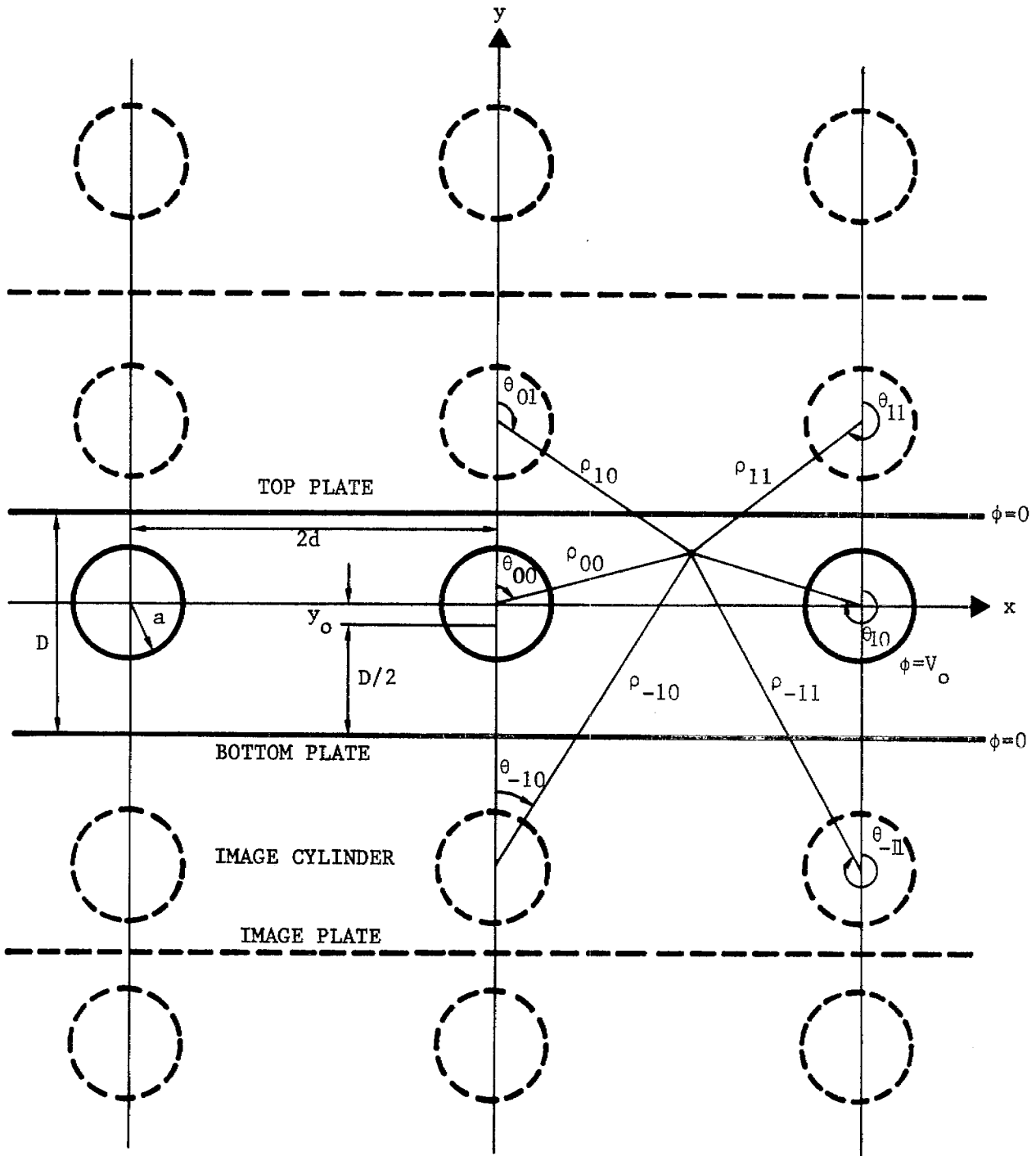
Figure 4. Two-dimensional electrostatic problem treated in section III.
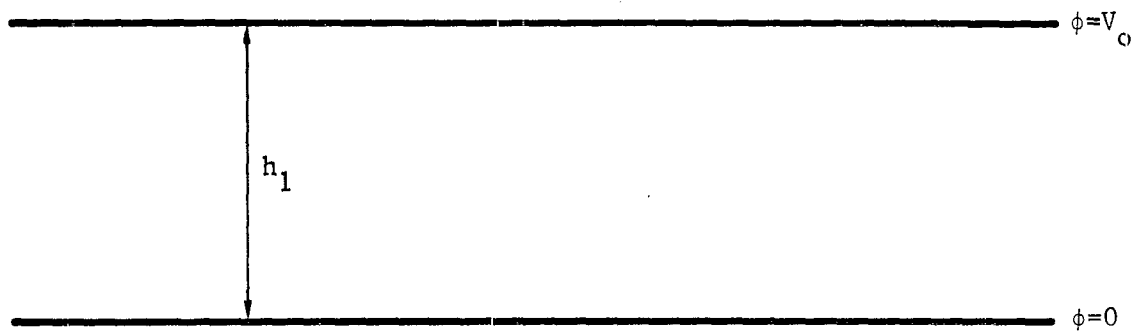
Figure 5. Effective electric height of transmission line treated in section II.
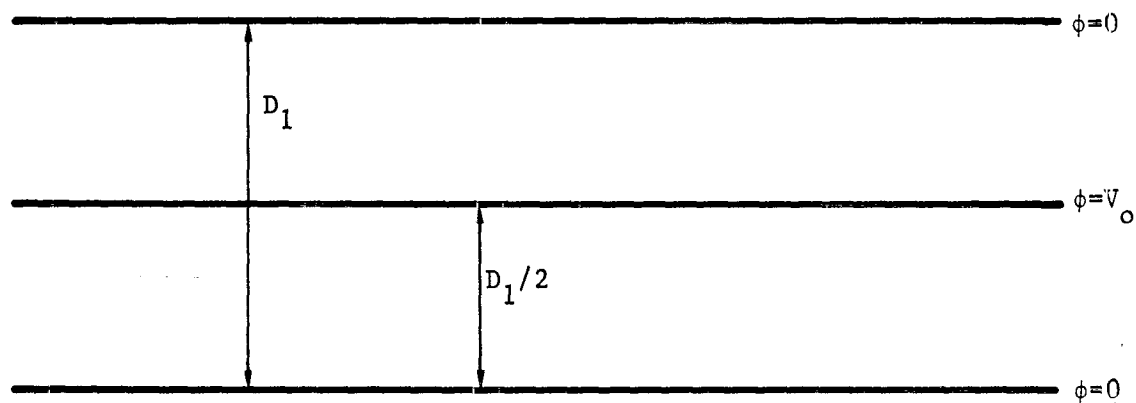


Figure 6. Effective electric height of transmission line treated in section III.
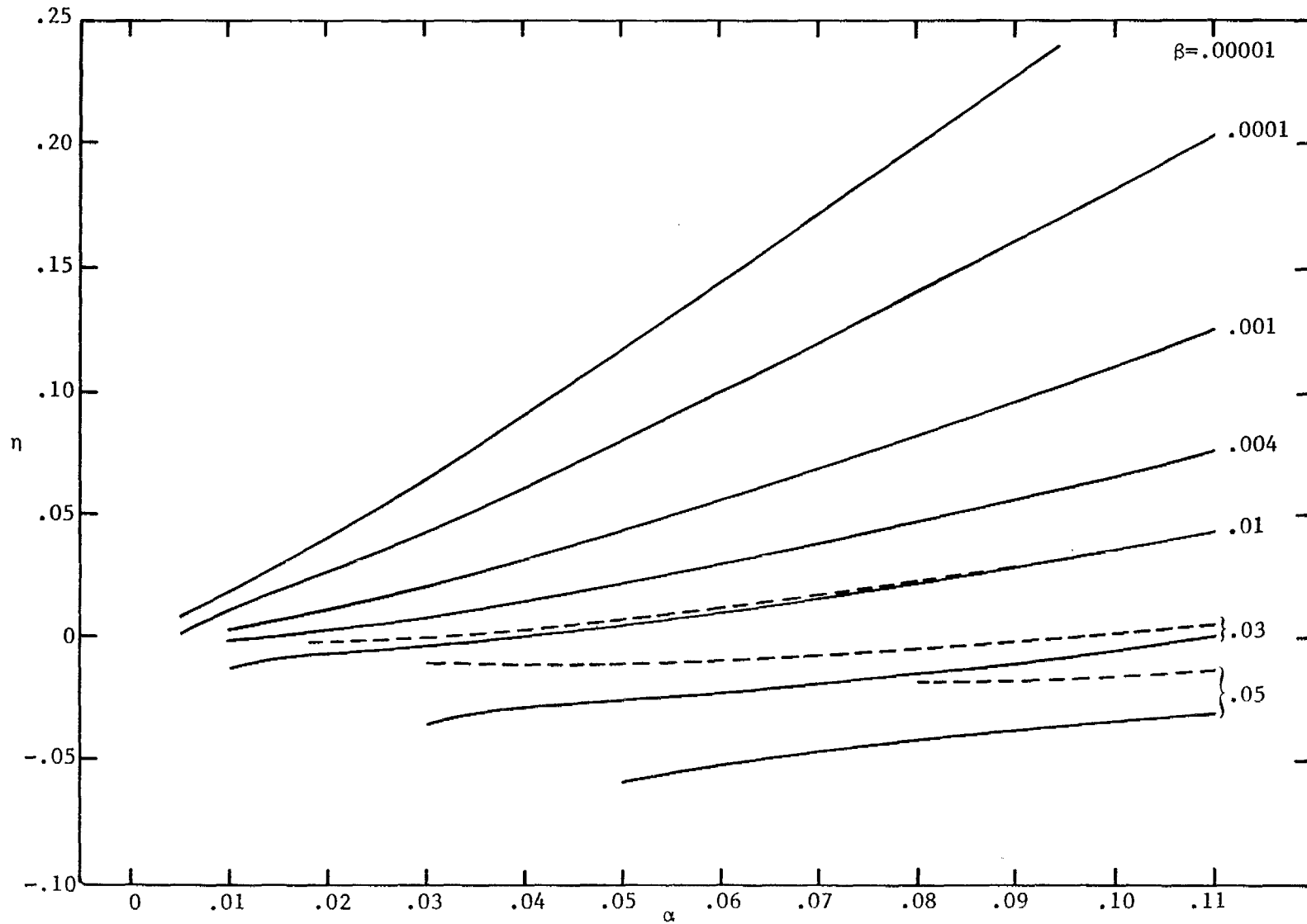
Figure 7. Effective electric height of transmission line treated in section II.
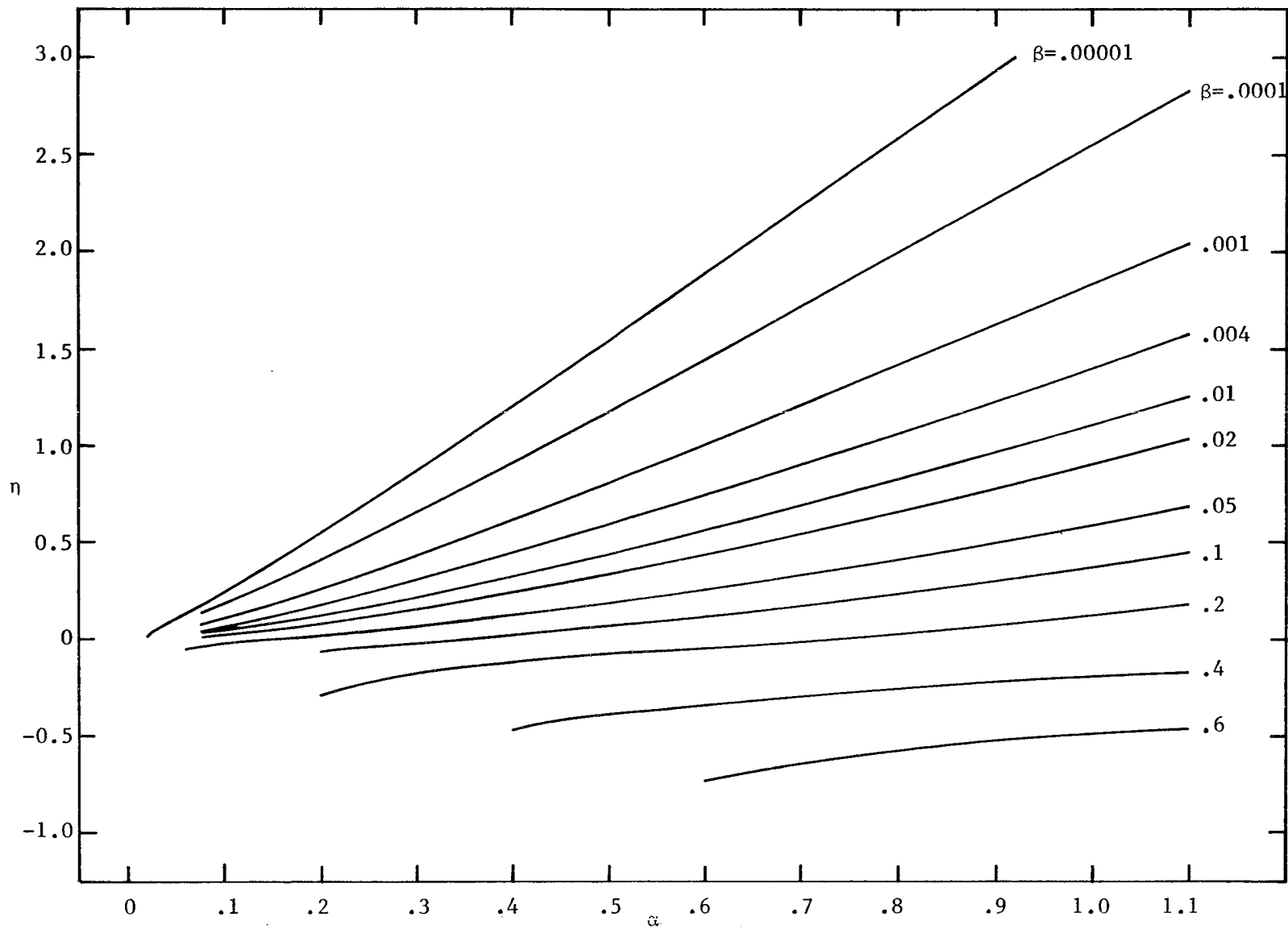
Figure 8. Effective electric height of transmission line treated in section II.
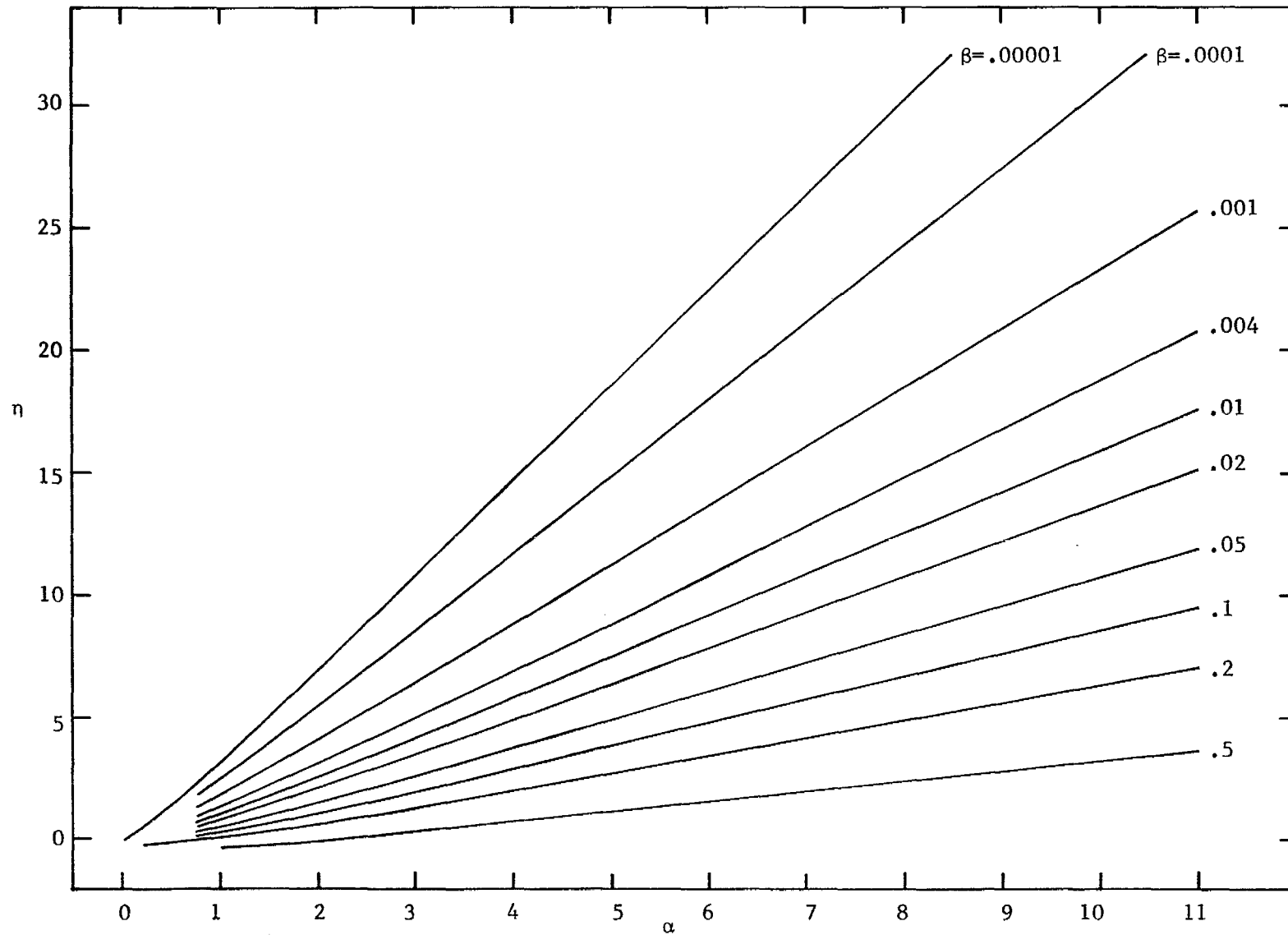
Figure 9. Effective electric height of transmission line treated in section II.
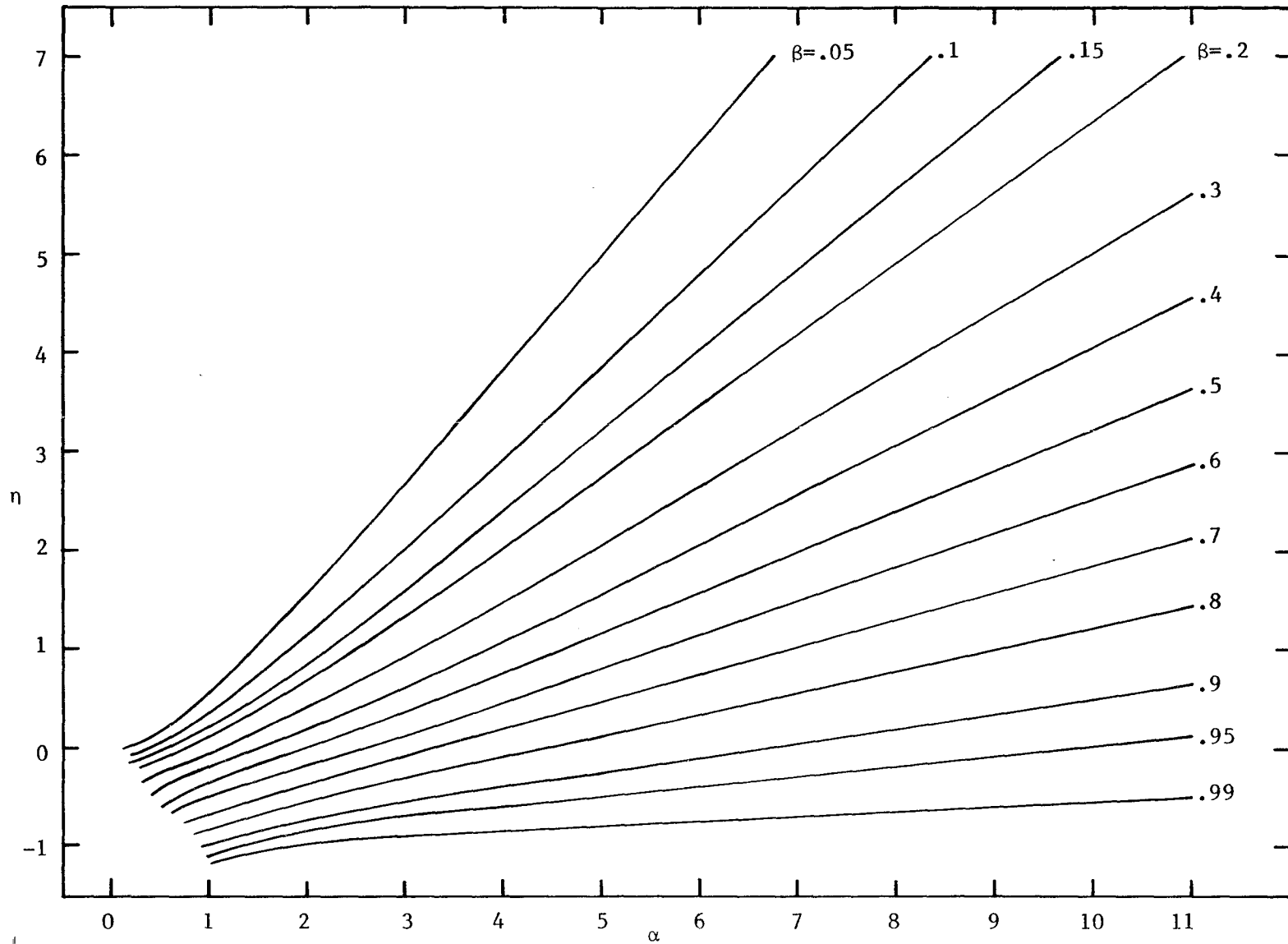
Figure 10. Effective electric height of transmission line treated in section II.
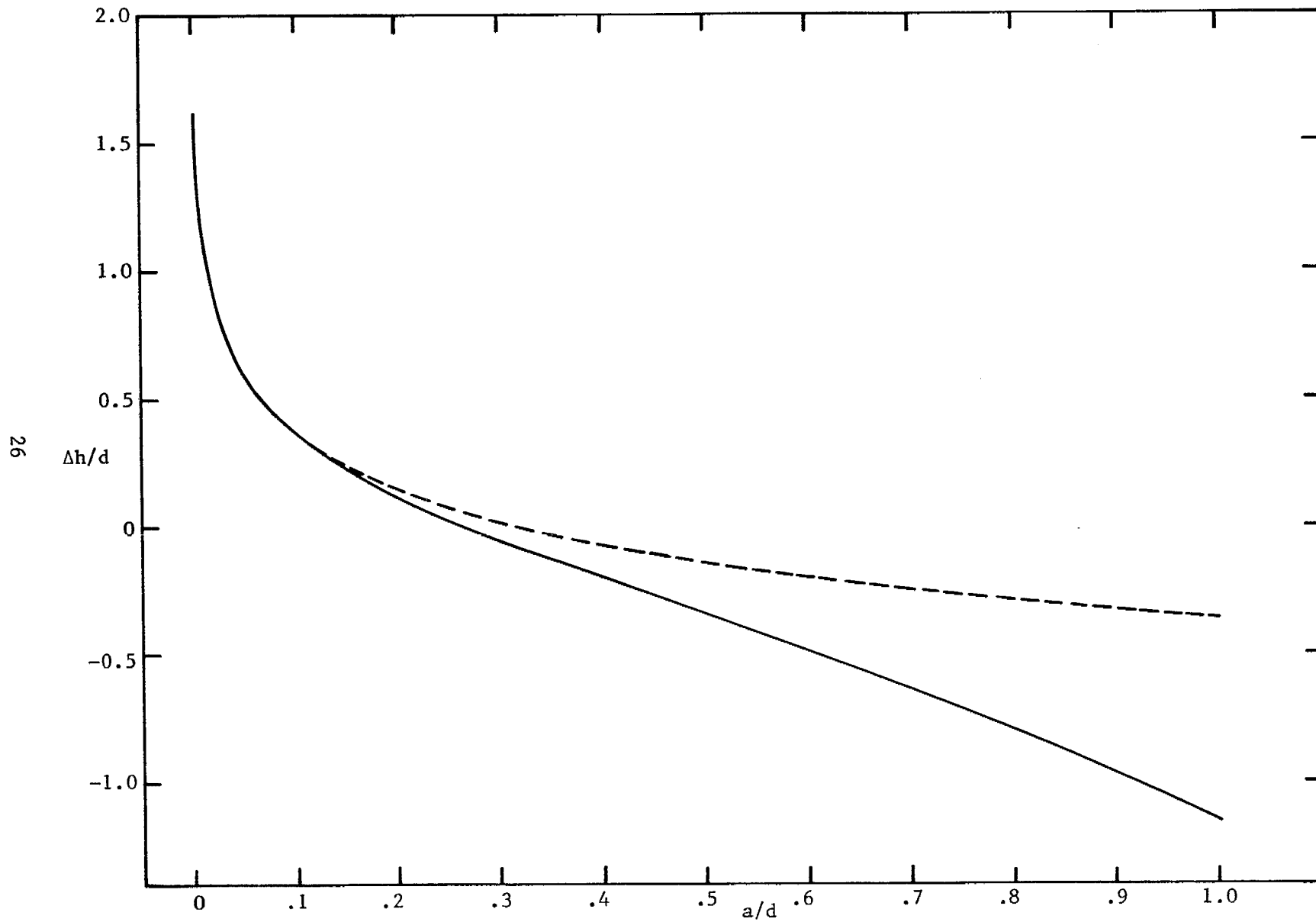
Figure 11.  Limit value as h tends to infinity of incremental electric height of transmission line treated in section II.
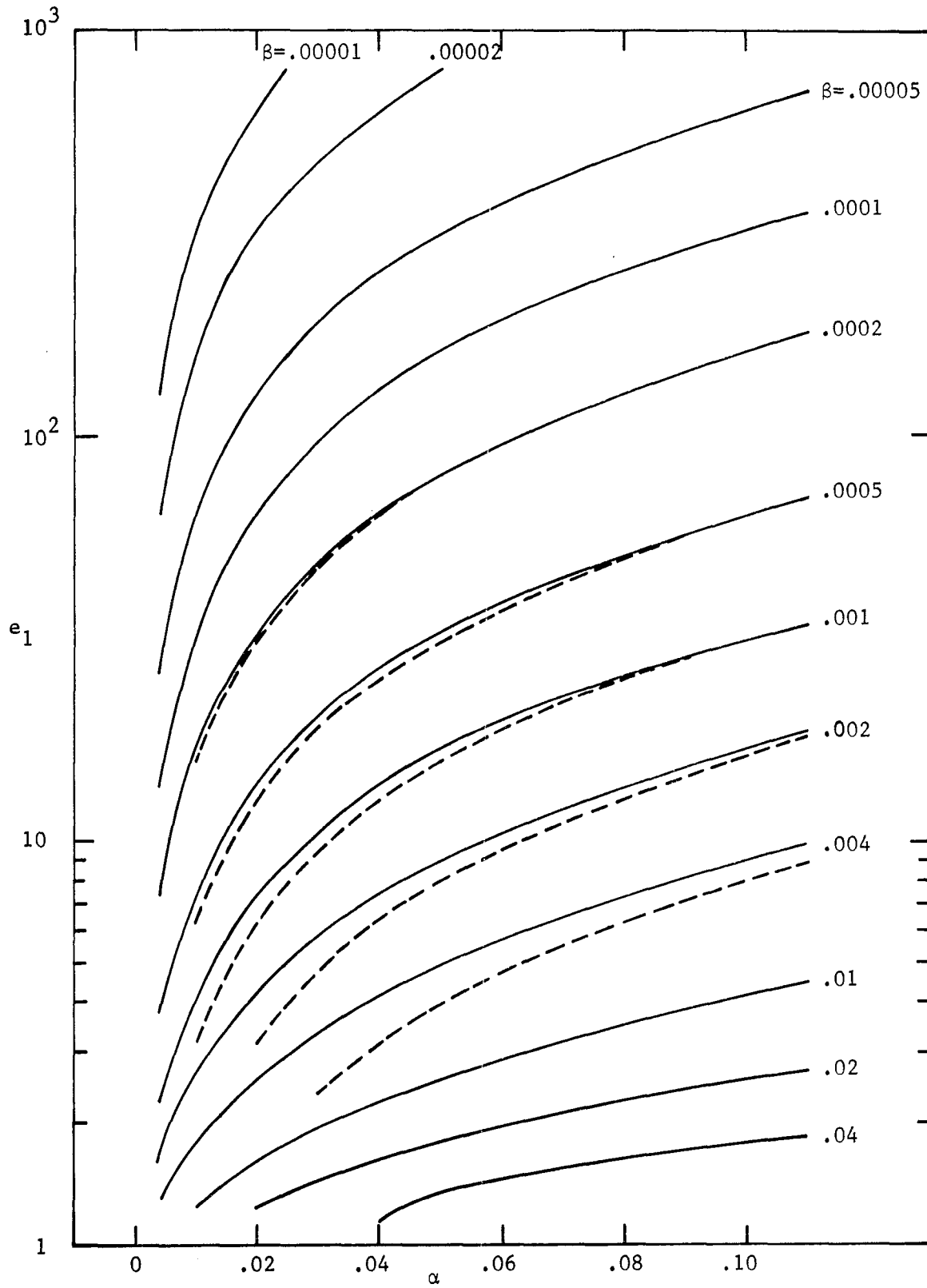
Figure 12.  Field enhancement factor of transmission line treated
in section II.

27
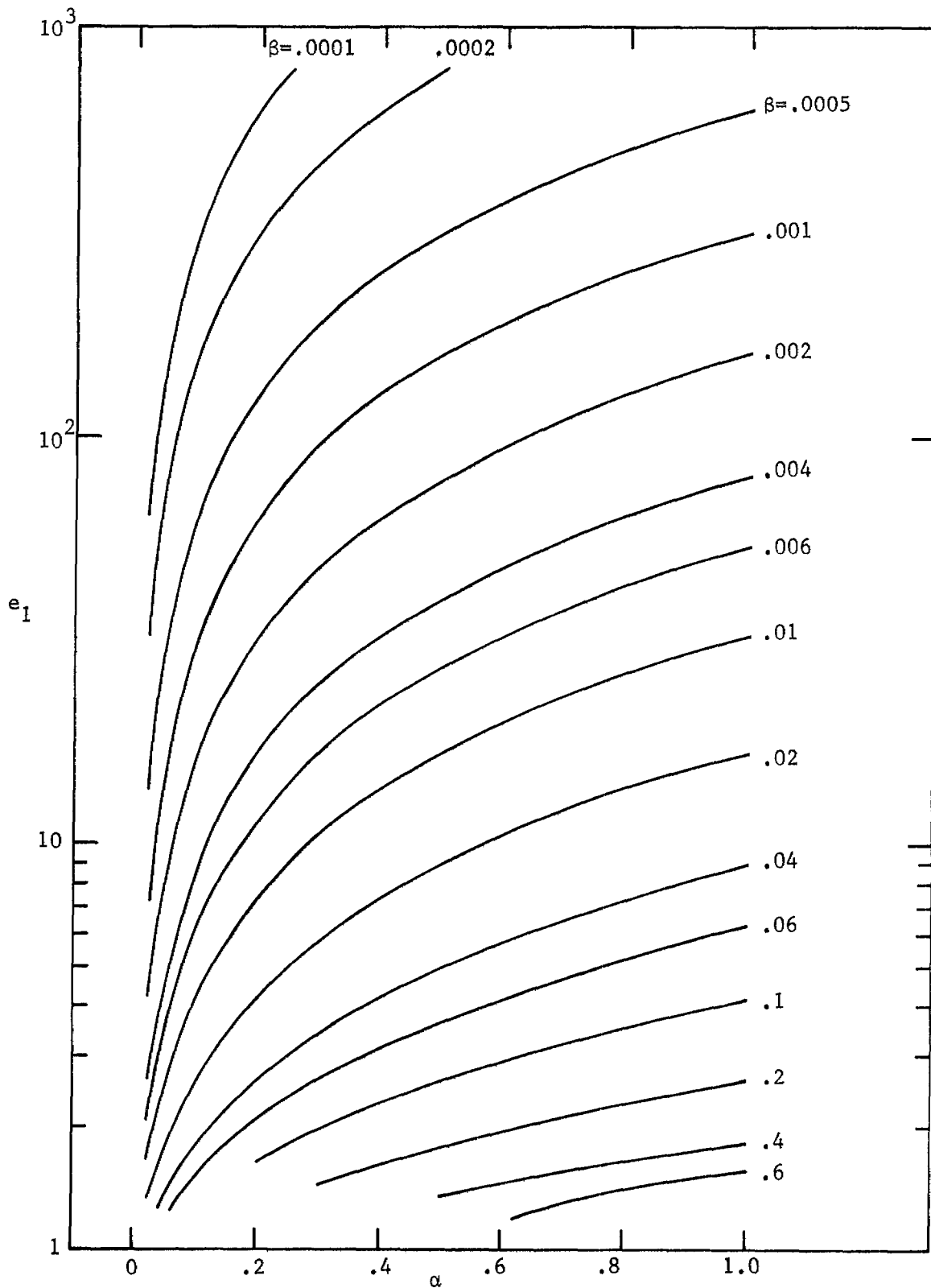
Figure 13.   Field enhancement factor of transmission line treated
in section II.

28
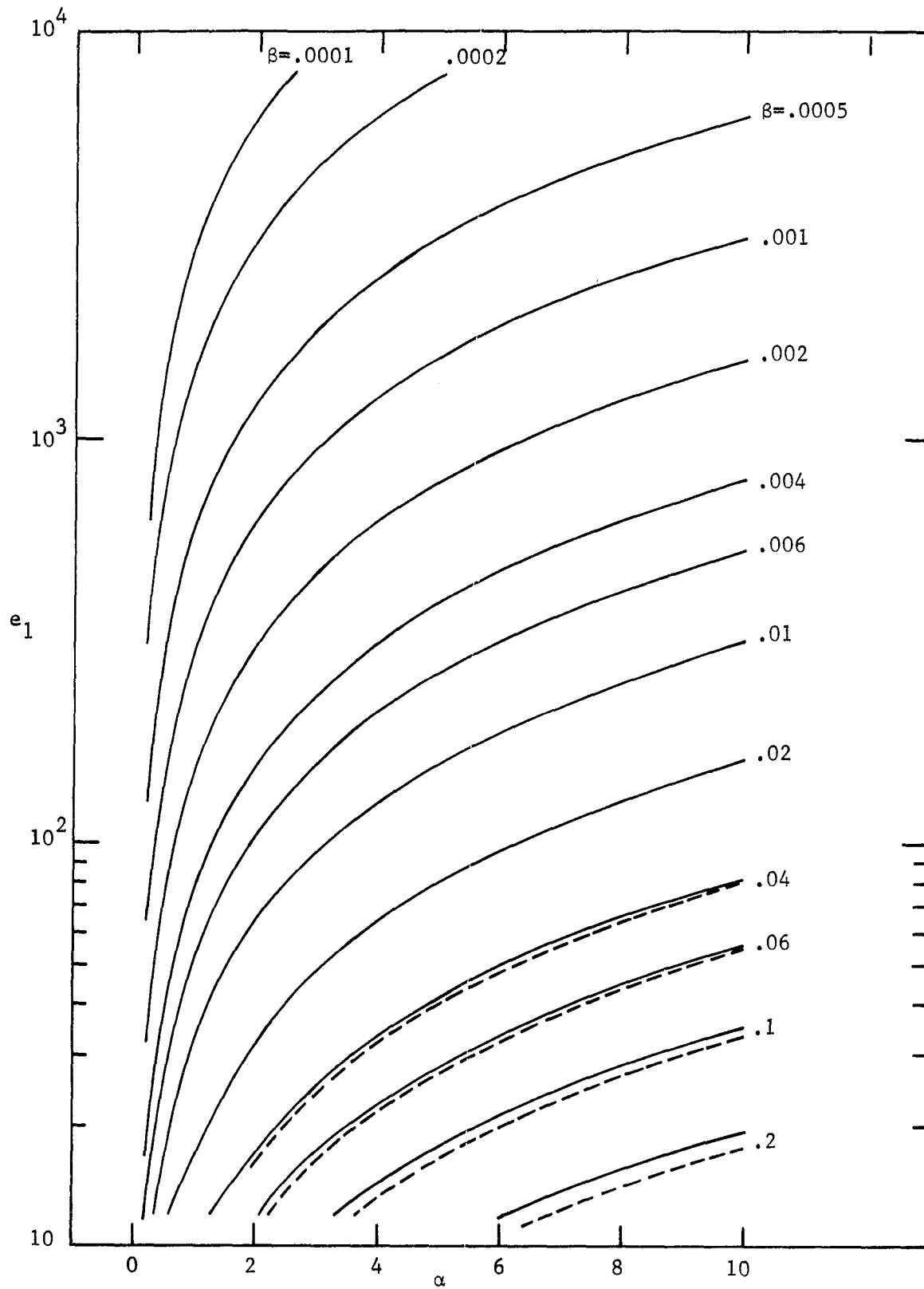
Figure 14.  Field enhancement factor of transmission line treated in section II.
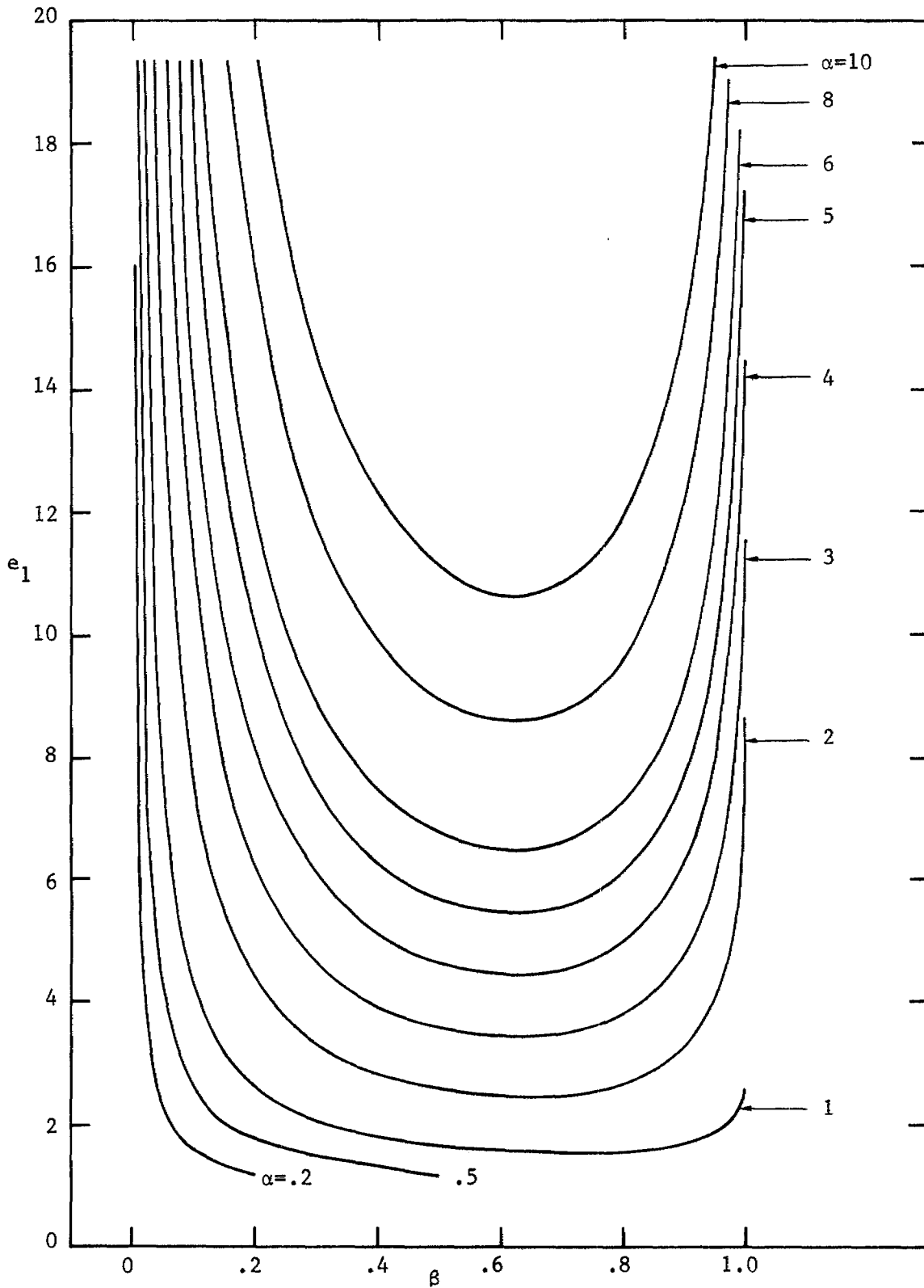
Figure 15. Field enhancement factor of transmission line treated in section II.
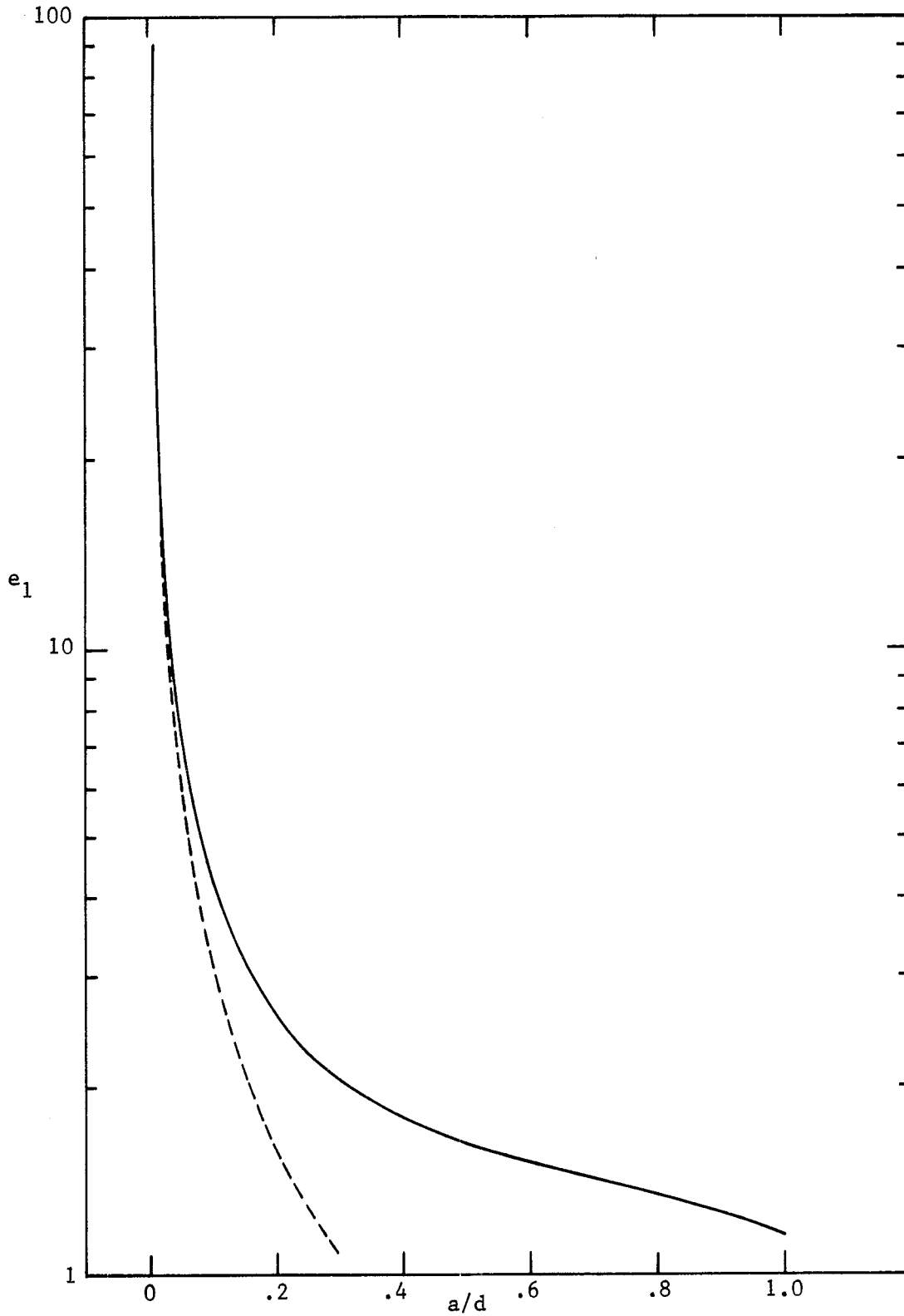
Figure 16. Limit value as h tends to infinity of field enhancement factor of transmission line treated in section II.
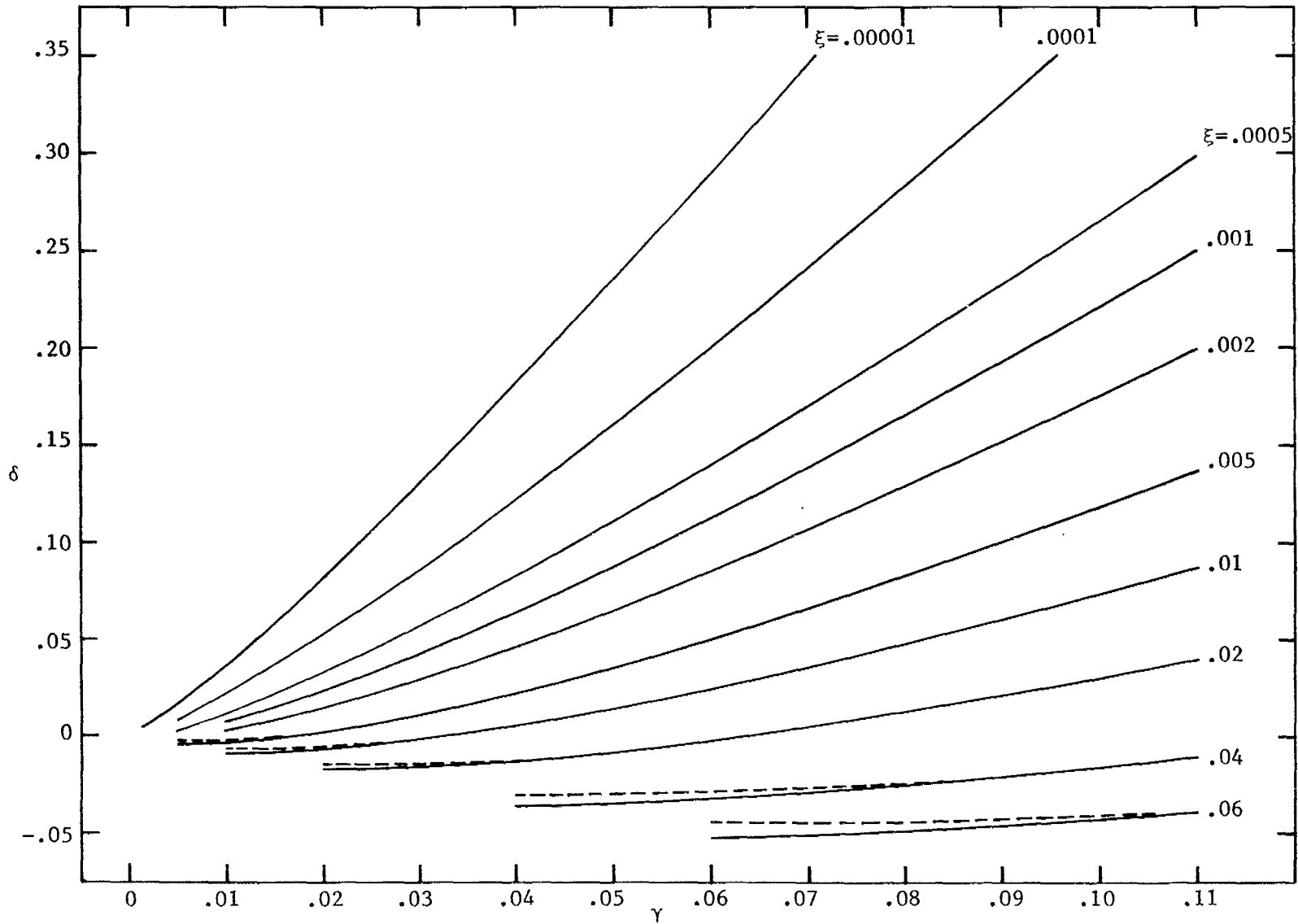
Figure 17. Effective electric height of transmission line treated in section III.
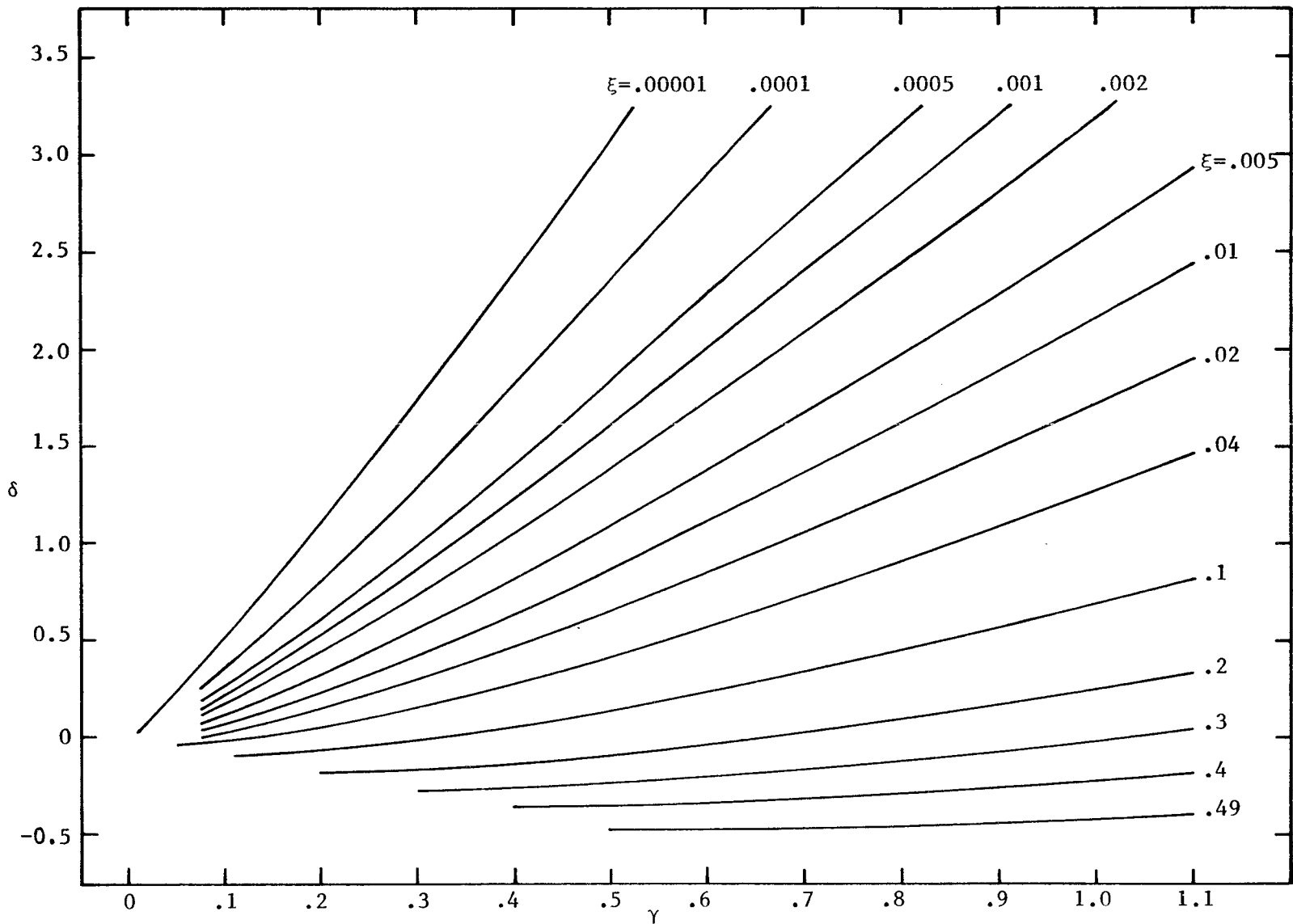
Figure 18.   Effective electric height of transmission line treated in section III.
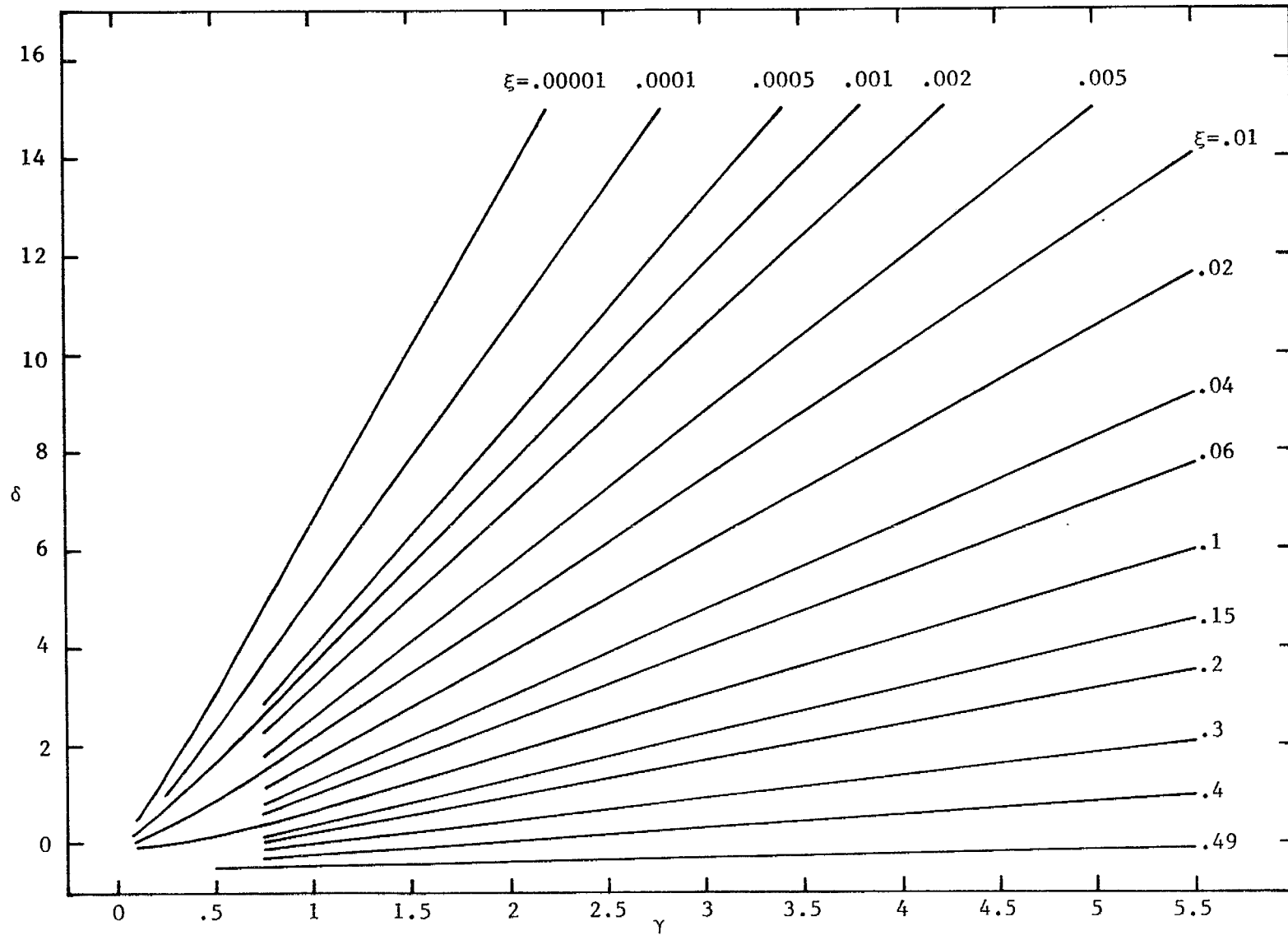
Figure 19. Effective electric height of transmission line treated in section III.
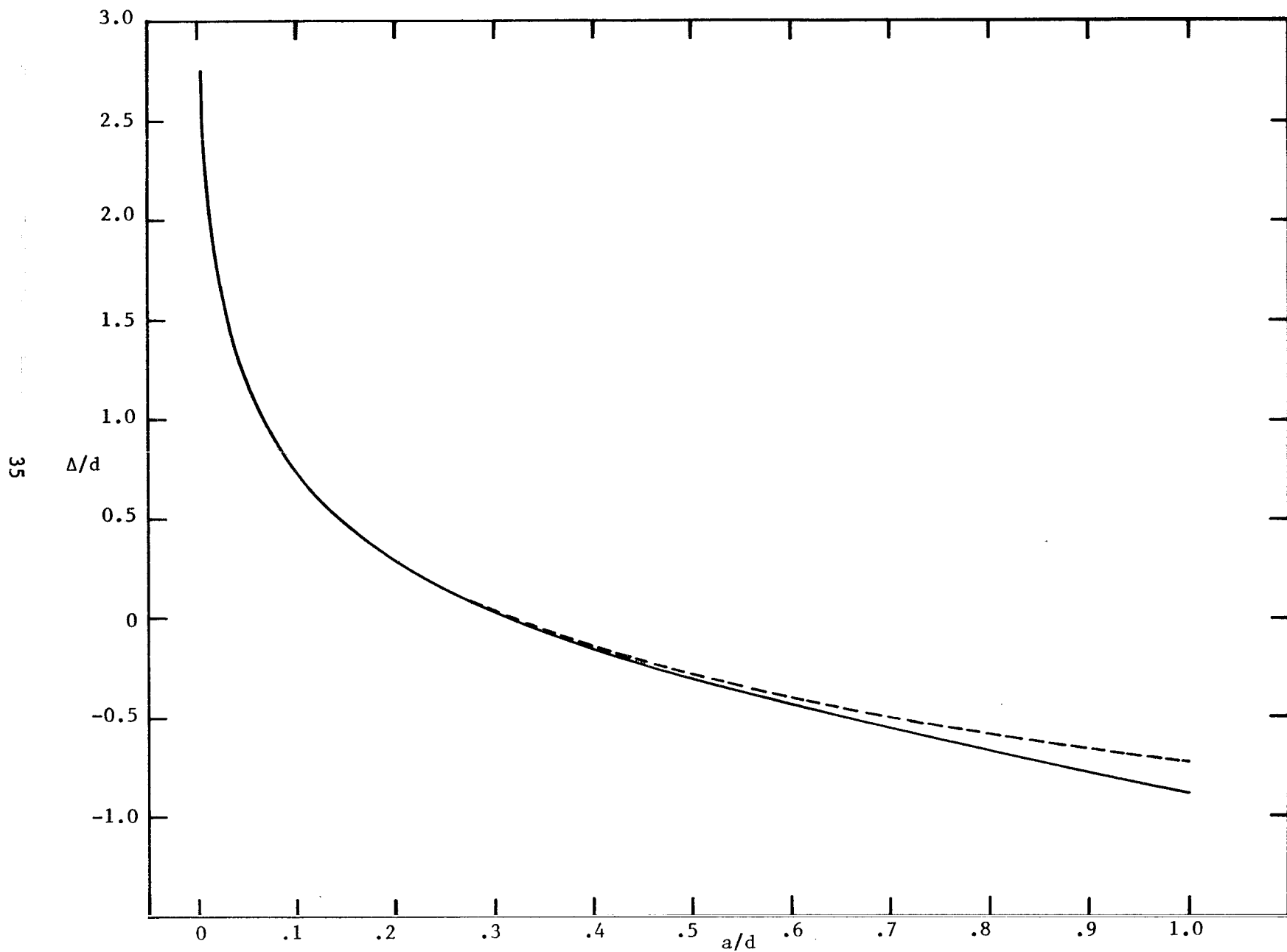
Figure 20. Limit value as D tends to infinity of incremental electric height of transmission line treated in section III.
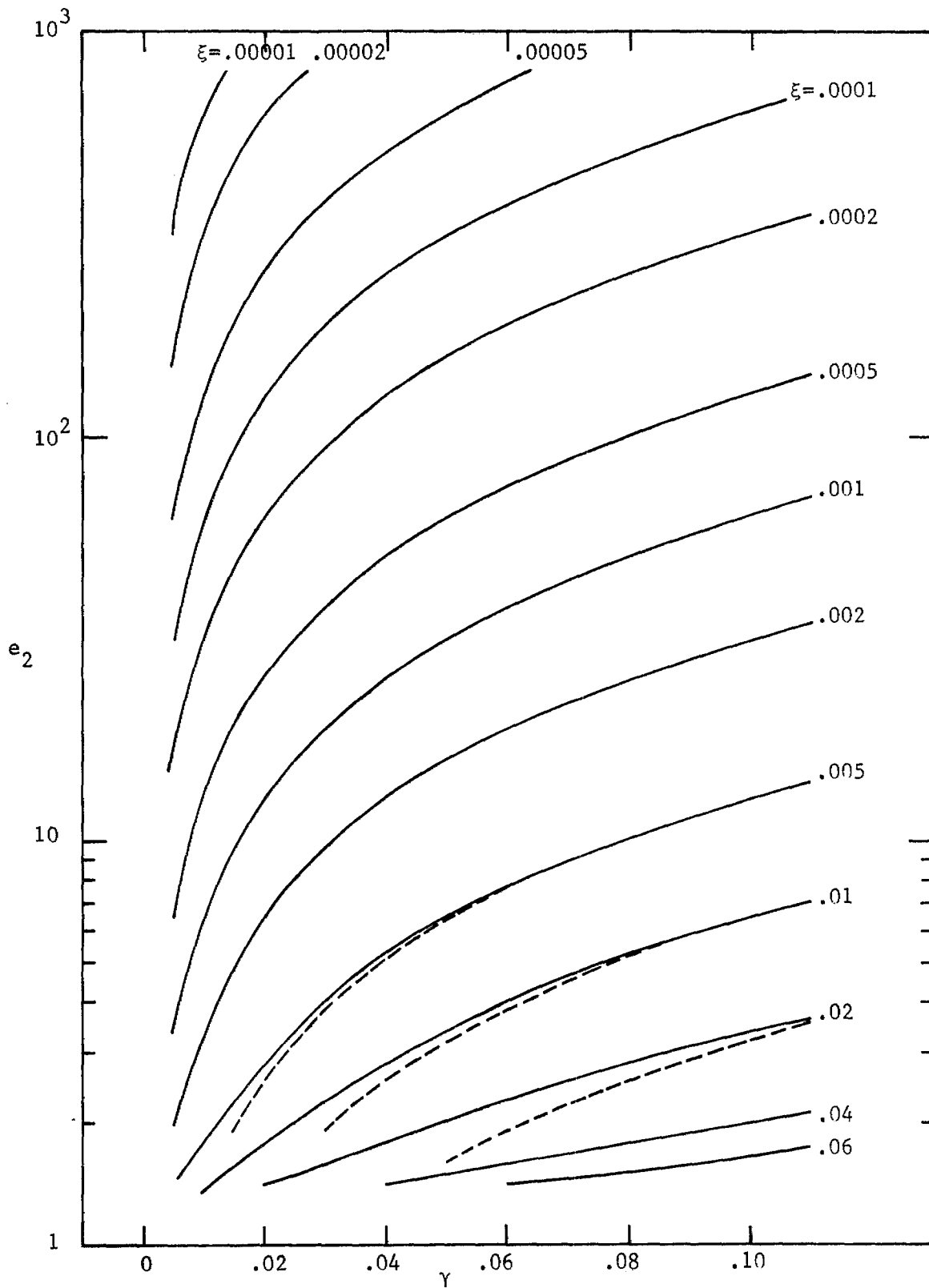
Figure 21. Field enhancement factor of transmission line treated in section III.
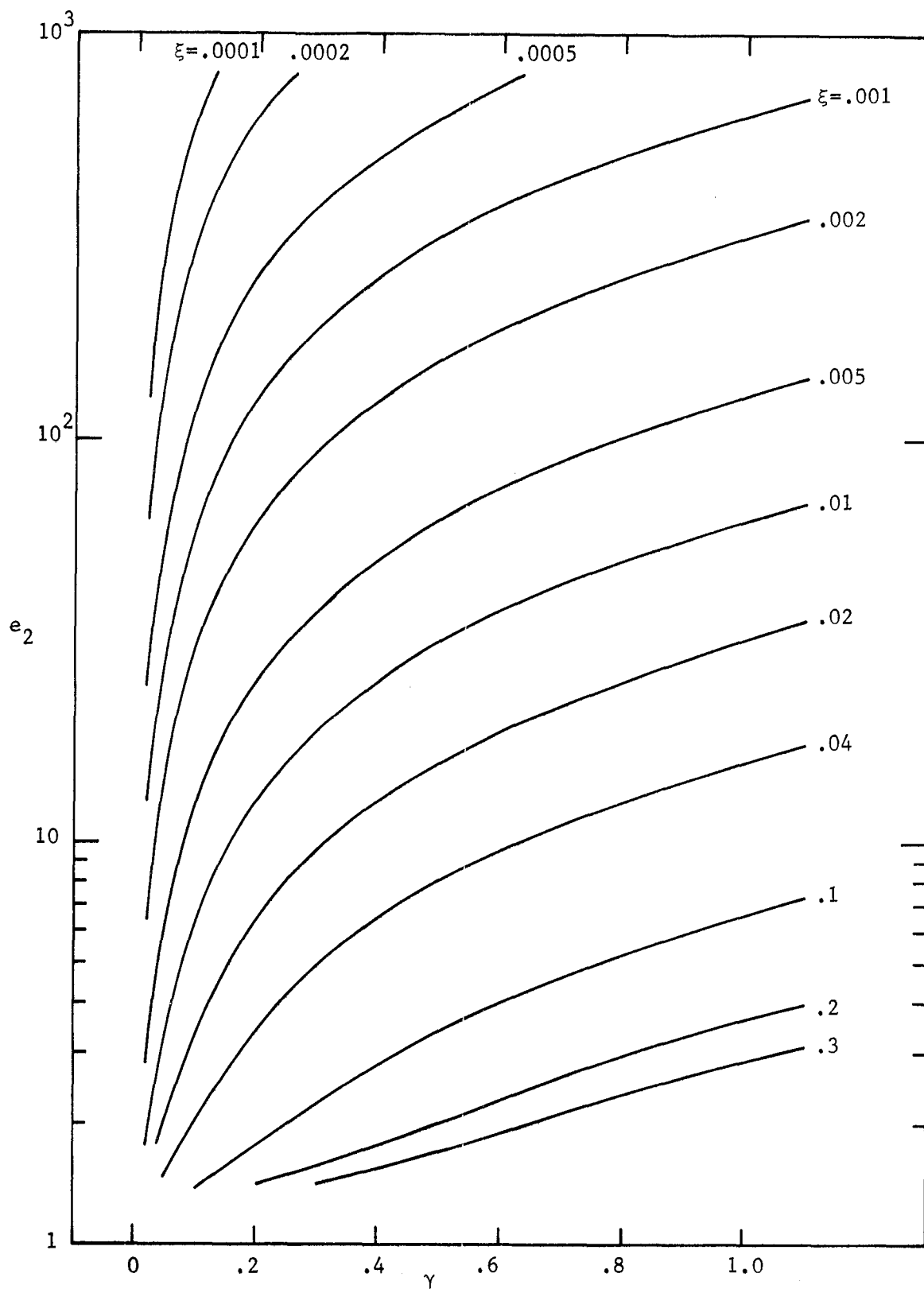
Figure 22.   Field enhancement factor of transmission line treated
in section III.

37
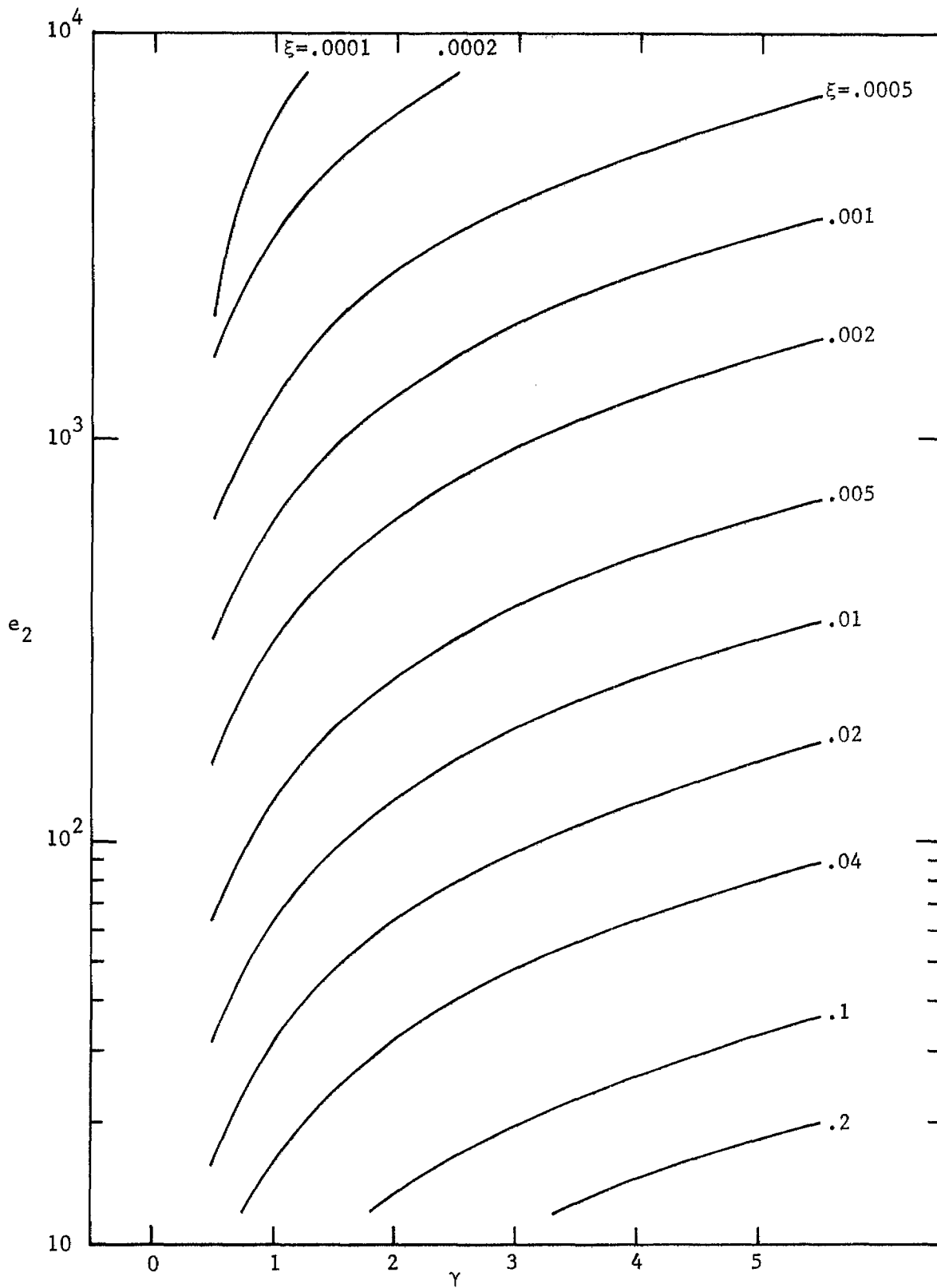
Figure 23.   Field enhancement factor of transmission line treated
in section III.
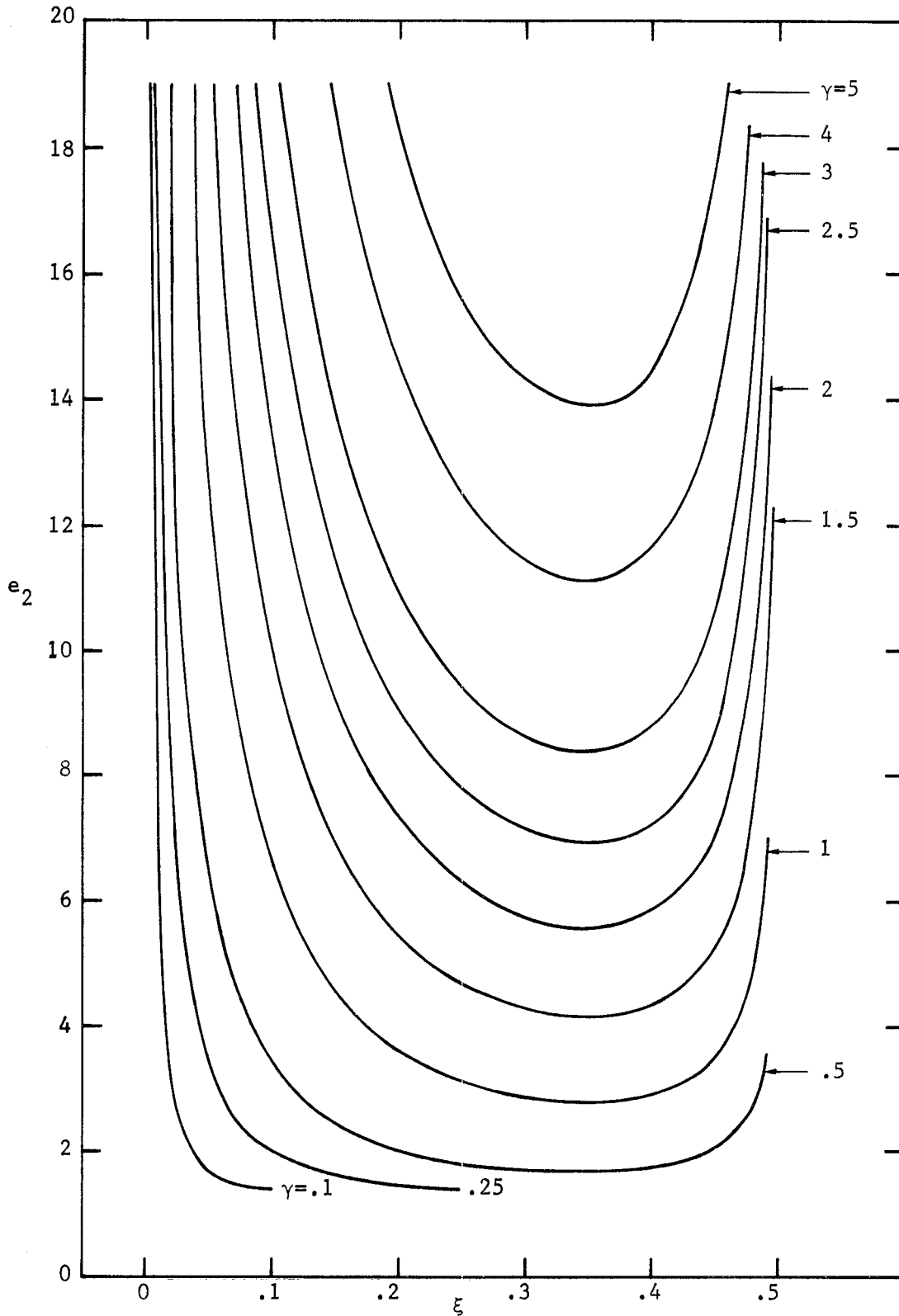
Figure 24.   Field enhancement factor of transmission line
treated in section III.
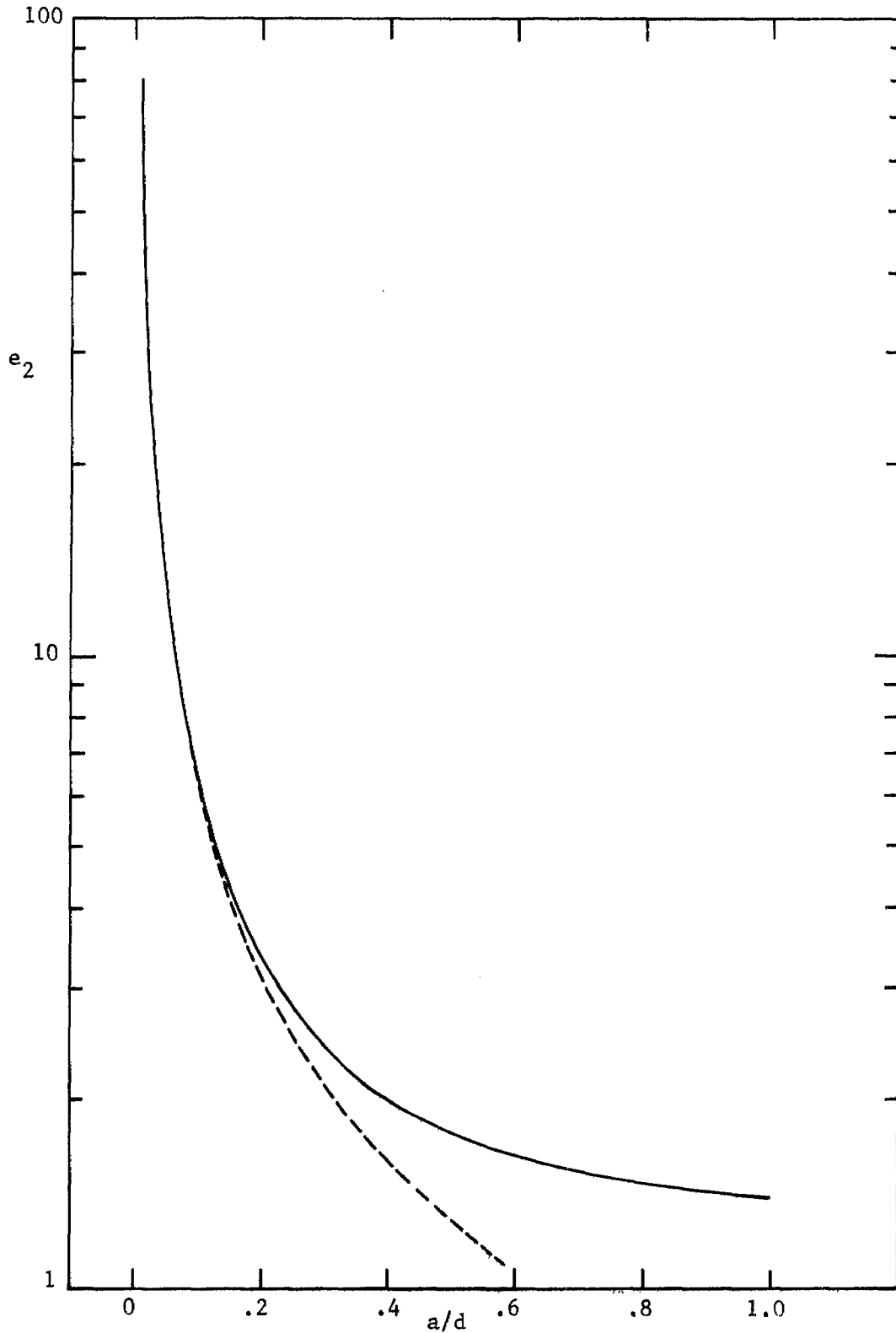
Figure 25. Limit value as D tends to infinity of field
enhancement factor of transmission line treated
in section III.

40

# Appendix A

## The Potential of a Lattice of Cylinders With Constant Charge Distribution

In this appendix we will derive some apparently different representations for the functions $g_e(x,y)$ and $g_i(x,y)$, defined by equations (19) and (20) in section III. Suppose the charge distribution, $\sigma_o(\theta_{ok})$, on each cylinder between the plates is constant so that

$$\sigma_o(\theta_{ok}) = s_o = \text{const.} \quad , \quad 0 \le \theta_{ok} \le 2\pi \quad . \tag{A1}$$

With $z = x + iy$ and making use of the conformal mappying $w = \exp(\pi z/D)$ we arrive at the following expressions for $g_e(x,y)$ and $g_i(x,y)$

$$g_e(x,y) = - as_o\varepsilon_o^{-1} \sum_{k=-\infty}^{\infty} \ln\left|\tanh[\tfrac{1}{2}\pi(z - 2kd)/D]\right| \quad , \tag{A2}$$

$$g_i(x,y) = as_o\varepsilon_o^{-1} \ln|z/a| - as_o\varepsilon_o^{-1} \sum_{k=-\infty}^{\infty} \ln\left|\tanh[0.5\,\pi(z - 2kd)/D]\right| \tag{A3}$$

and

$$g_i(0,0) = as_o\varepsilon_o^{-1} \ln(2Da^{-1}\pi^{-1}) - 2as_o\varepsilon_o^{-1} \sum_{k=1}^{\infty} \ln\tanh[\pi kd/D] \quad . \tag{A4}$$

Introducing the conformal mapping $w = \exp(i\pi z/d)$ and making use of the method of images we get

$$g_e(x,y) =$$

$$as_o\varepsilon_o^{-1} \sum_{k=1}^{\infty} \ln\left|(1 - w^{-1}v^{-4k+2})(1 - wv^{-4k+2})(1 - w^{-1}v^{-4k})^{-1}(1 - wv^{-4k+4})^{-1}\right|$$

$$+ \frac{1}{2} as_o\varepsilon_o^{-1} \ln|wv| \quad , \tag{A5}$$

$$g_i(x,y) =$$

$$as_o\varepsilon_o^{-1} \sum_{k=1}^{\infty} \ln\left|(1 - w^{-1}v^{-4k+2})(1 - wv^{-4k+2})(1 - w^{-1}v^{-4k})^{-1}(1 - wv^{-4k+4})^{-1}\right|$$

$$+ as_o\varepsilon_o^{-1} \ln|wv| + \frac{1}{2} as_o\varepsilon_o^{-1} \ln|z/a| \tag{A6}$$

where $v = \exp(\pi D/2d)$. Moreover, we have

$$g_i(0,0) = as_o\varepsilon_o^{-1}\left[\pi D(4d)^{-1} + \ln(d\pi^{-1}a^{-1}) - \sum_{k=1}^{\infty} (-1)^k \ln(1 - e^{-\pi kD/d})\right] . \tag{A7}$$

The two expressions, (A4) and (A7), for $g_i(0,0)$, although seemingly different, are identical as can be seen from the analysis below.

Consider the function $f(\gamma)$ defined by

$$f(\gamma) = \sum_{k=1}^{\infty} \ln \tanh(\pi\gamma k) \tag{A8}$$

$$f'(\gamma) = \sum_{k=1}^{\infty} 2\pi k/\sinh(2\pi\gamma k) \quad . \tag{A9}$$

Making use of the Poisson summation formula we get

$$f'(\gamma) = -\frac{1}{2}\gamma^{-1} + (\pi/8)\gamma^{-2} - \pi\gamma^{-2} \sum_{k=1}^{\infty} [(-1)^k k e^{-\pi k/\gamma}][1 - e^{-\pi k/\gamma}]^{-1} \tag{A10}$$

and

$$f(\gamma) = -\frac{1}{2}\ln\gamma - \pi(8\gamma)^{-1} + \sum_{k=1}^{\infty} (-1)^k \ln(1 - e^{\pi k/\gamma}) + C \tag{A11}$$

where C is a constant of integration. Putting $\gamma = 1$ in equations (A8) and (A11) and identifying the two expressions for $f(1)$ thus derived we get

$$C = \pi/8 - \sum_{k=1}^{\infty} (-1)^k \ln[1 + (-1)^k e^{-\pi k}] \quad . \tag{A12}$$

From the theory of theta functions it follows that (see reference 4 chap. XXI)

42

$$\sum_{k=1}^{\infty} (-1)^k \ln[1 + (-1)^k e^{-\pi k}] = \frac{1}{2} \ln 2 + \pi/8 \qquad (A13)$$

and

$$C = \frac{1}{2} \ln 2 \quad . \qquad (A14)$$

Thus,

$$\sum_{k=1}^{\infty} \ln \tanh(\pi \gamma k) = \frac{1}{2} \ln(2/\gamma) - \pi(8\gamma)^{-1} + \sum_{k=1}^{\infty} (-1)^k \ln(1 - e^{-\pi k/\gamma}) \qquad (A15)$$

and it is easy to see that the two expressions (A4) and (A7) for $g_i(0,0)$ are identical.

## Appendix B
### Some Special Cases

For pedagogial reasons we will here consider three special cases all of which can be obtained by taking proper combinations of limits of the problems treated in sections II and III. In case 1 we consider a grid of rods supporting a uniform field on one side of the rods. This case can be obtained by letting h tend to infinity in the problem treated in section II. In case 2 we consider a grid of rods supporting a uniform field of equal magnitude but opposite direction on the two sides of the grid. This case can be obtained by letting D tend to infinity in the problem treated in section III. In case 3 we consider a grid of rods supporting a uniform field of equal magnitude and same direction on the two sides sides of the rods. This case can be obtained by superposing the results of case 1 and 2.

From the symmetry of the problem it follows that we can make the following Fourier series expansion of the charge distribution, $\sigma(\theta_k)$, on the cylinder with center at x = 2kd, (... -2, -1, 0, 1, 2, ...) and y = 0

$$\sigma(\theta_k) = \sum_{n=0}^{\infty} s_n \cos n\theta_k \quad . \tag{B1}$$

Outside the cylinders we have the potential

$$\phi_{ep}(x,y) = h_{ep}(x,y) + \sum_{n=1}^{\infty} \sum_{k=-\infty}^{\infty} \frac{a s_{np}}{2n\epsilon_o} \left(\frac{a}{\rho_k}\right)^n \cos n\theta_k \tag{B2}$$

where $\rho_k$ and $\theta_k$ are defined in figure 26 and p = 1, 2 and 3 denotes case 1, 2 and 3, respectively. In case 1 and 2 the function $h_{ep}(x,y)$ is the potential due to the net charges on the cylinders having the asymptotic value $h_p(x,y)$, p = 1 and 2, where

$$\frac{dh_1}{dy} = \begin{cases} E_1 & , \quad y < 0 \\ \\ 0 & , \quad y > 0 \end{cases} \tag{B3}$$

and

$$\frac{dh_2}{dy} = - E_2 \, \text{sgn}(y) \tag{B4}$$

as $|y| \to \infty$. With $z = x + iy$ and introducing the conformal mappings $w = \exp(i\pi z/d)$ and $w = \sin(\pi z/2d)$ in case 1 and 2 respectively we arrive at the following expressions

$$h_{e1}(x,y) = - dE_1 (2\pi)^{-1} \ln[1 + e^{-2\pi y/d} - 2e^{-\pi y/d} \cos(\pi x/d)] \qquad (B5)$$

and

$$h_{e2}(x,y) = - dE_2 \pi^{-1} \ln[\sin^2(\pi x/2d)\cosh^2(\pi y/2d) + \cos^2(\pi x/2d)\sinh^2(\pi y/2d)]. \quad (B6)$$

The function $h_{e3}(x,y)$ represents a homogeneous incident field,

$$h_{e3}(x,y) = - E_3 y \quad . \tag{B7}$$

Inside one of the cylinders, e.g. the 0-th cylinder, we have the potential

$$\phi_{ip}(x,y) = h_{ip}(x,y) + \sum_{n=1}^{\infty} \sum_{k=-\infty}^{\infty}{}' \frac{a s_{np}}{2n\varepsilon_0} \left(\frac{a}{\rho_k}\right)^n \cos n\theta_k$$

$$+ \sum_{n=1}^{\infty} \frac{a s_{np}}{2n\varepsilon_0} \left(\frac{\rho_0}{a}\right)^n \cos n\theta_0 \quad , \quad p = 1,2,3 \qquad (B8)$$

where

$$h_{i1}(x,y) = - dE_1 (2\pi)^{-1} \ln\{[1 + e^{-2\pi y/d} - 2e^{-\pi y/d} \cos(\pi x/d)]a^2/(x^2 + y^2)\} \quad ,$$

$$h_{i2}(x,y) = - dE_2 \pi^{-1} \ln\{[\sin^2(\pi x/2d)\cosh^2(\pi y/2d)$$

$$+ \cos^2(\pi x/2d)\sinh^2(\pi y/2d)]a^2/(x^2 + y^2)\} \quad ,$$

$$h_{i3}(x,y) = - E_3 y$$

and the prime on the summation indicates omission of the $k = 0$ term.

Putting the potential on each cylinder equal to a constant $(V_p)$ and using the method described on page 5 in section II we arrive at the system of equations

$$V_p = h_{ep}(0,0) + \sum_{n=1}^{\infty} \sum_{k=1}^{\infty} \frac{as_{np}}{n\varepsilon_o} \left(\frac{a}{2kd}\right)^n \cos \frac{n\pi}{2}$$

(B9)

$$0 = h_{ep}^{(\ell)}(0,0) + \frac{as_{ep}}{2\varepsilon_o}$$
$$+ \sum_{n=1}^{\infty} \sum_{k=1}^{\infty} \frac{as_{np}}{n\varepsilon_o} (-1)^{\ell} \binom{\ell+n-1}{n} \left(\frac{a}{2kd}\right)^{\ell+n} \cos \frac{(\ell+n)\pi}{2} \quad , \quad \ell \geq 1$$

where

$$h_{ep}^{(\ell)}(x,y) = \frac{a^{\ell}}{(\ell-1)!} \frac{\partial^{\ell} h_{ep}}{\partial y^{\ell}} (x,y) \quad , \quad \ell \geq 1 \quad .$$

We have, trivially,

$$h_{e3}(0,0) = 0 \quad ,$$

(B10)

$$h_{e3}^{(\ell)}(0,0) = - aE_3 \delta_{\ell 1} \quad , \quad \ell \geq 1$$

and

$$h_{ep}(0,0) = pdE_p \pi^{-1} \ln(pd/a\pi) \quad , \quad p = 1,2 \quad . \tag{B11}$$

From the definition of the Bernoulli numbers it follows that for $p = 1,2$ we have

$$h_{ep}^{(1)}(0,0) = 0.5 \, aE_p \delta_{1p} \tag{B12}$$

and

$$h_{ep}^{(\ell)}(0,0) = \begin{cases} 0 \quad , & \ell \text{ odd and } \ell \geq 3 \\ \\ paE_p (\pi a/d)^{\ell-1} (-1)^{\ell/2} B_{\ell/2}/\ell! \quad , & \ell \text{ even and } \ell \geq 2 \end{cases} \tag{B13}$$

46

From the above it follows that

$$s_{n2} = 0 \quad , \quad n \text{ odd}$$

(B14)

$$s_{n3} = 0 \quad , \quad n \text{ even} \quad .$$

Moreover, putting $E_1 = E_2 = E_3$ the solutions $s_{np}$ of equation (B9) are linearly dependent,

$$s_{n3} = s_{n2} - 2s_{n1} \quad .$$

(B15)

Notice also that equation (B9) with p = 1 can be obtained as the limit of equation (6) in section II as h tends to infinity and that equation (B9) with p = 2 can be obtained as the appropriate limit of equation (22) in section III as D tends to infinity.

For $y \to - \infty$ we have the potential

$$\phi_{ep}(x,y) = E_p y \, \text{sgn}(2.5 - p) + \pi a^2 (4d\varepsilon_o)^{-1} s_{1p}$$

$$+ E_p \delta_{2p} 2d\pi^{-1} \ln 2 + O(y^{-1}) \quad , \quad p = 1,2,3 \quad .$$

(B16)

The effective electric position of the grid as defined in reference 1 page 30, is given by

$$y = \Delta_p = [V_p - E_p \delta_{2p} 2d\pi^{-1} \ln 2 - \pi a^2 (4d\varepsilon_o)^{-1} s_{1p}]/E_p \, \text{sgn}(2.5 - p) \quad , \quad p = 1,2,3 \quad .$$

(B17)

From equations (B9) and (B17) it follows that

$$\Delta_3 = 2\Delta_1 - \Delta_2 \quad .$$

(B18)

For d >> a we have

$$\Delta_1 \approx \Delta_1' = d\pi^{-1} \ln(d\pi^{-1}a^{-1}) - \pi a^2/(4d) \quad ,$$

$$\Delta_2 \approx \Delta_2' = 2d\pi^{-1} \ln(d\pi^{-1}a^{-1}) \tag{B19}$$

and

$$\Delta_3 \approx \Delta_3' = -0.5 \pi a^2/d \quad .$$

The field enhancement factor is

$$e_p(\theta_k) = \sigma_p(\theta_k)\varepsilon_o^{-1}E_p^{-1} \tag{B20}$$

and

$$e_p = \max_{\theta_k}\{|e_p(\theta_k)|\} = |\varepsilon_o^{-1}E_p^{-1} \sum_{n=0}^{\infty} (-1)^n s_{np}| \quad , \quad p = 1,2,3 \quad . \tag{B21}$$

From equations (B9) and (B21) it follows that

$$e_3 = 2e_1 - e_2 \quad . \tag{B22}$$

For $d \gg a$ we have

$$e_1 \approx e_1' = d\pi^{-1}a^{-1} + 1 \quad ,$$

$$e_2 \approx e_2' = 2d\pi^{-1}a^{-1} \tag{B23}$$

and

$$e_3 \approx e_3' = 2 \quad .$$

The quantities $\delta_p$,

$$\delta_p = \Delta_p d^{-1} \quad , \tag{B24}$$

and $e_p$ are tabulated in table 1 and graphed in figures 27 and 28. The broken curves in figure 27 correspond to the asymptotic values $\Delta_2'$ and $\Delta_3'$ given by equation (B19). The difference between $\Delta_1$ and $\Delta_1'$ is negligable for $0 < a < d$.

The broken curves in figure 28 correspond to the asymptotic values $e_2'$ and $e_3'$ given by equation (B23). The difference between $e_1$ and $e_1'$ is negligable for $0 < a < d$.

Table 1

| a/d | $\delta_1$ | $\delta_2$ | $\delta_3$ | $e_1$ | $e_2$ | $e_3$ |
|-----|-----------|-----------|-----------|--------|---------|--------|
| .02 | .88054 | 1.76171 | −.00063 | 16.9155 | 31.8519 | 1.9791 |
| .04 | .65896 | 1.32044 | −.00252 | 8.9577 | 15.9574 | 1.9580 |
| .06 | .52833 | 1.06231 | −.00565 | 6.3051 | 10.6731 | 1.9371 |
| .08 | .43456 | .87916 | −.01004 | 4.9788 | 8.0414 | 1.9162 |
| .10 | .36070 | .73709 | −.01569 | 4.1830 | 6.4707 | 1.8953 |
| .12 | .29921 | .62100 | −.02258 | 3.6524 | 5.4305 | 1.8743 |
| .14 | .24606 | .52283 | −.03071 | 3.2734 | 4.6934 | 1.8534 |
| .16 | .19884 | .43776 | −.04008 | 2.9891 | 4.1457 | 1.8325 |
| .18 | .15601 | .36269 | −.05067 | 2.7679 | 3.7242 | 1.8116 |
| .20 | .11651 | .29550 | −.06249 | 2.5909 | 3.3910 | 1.7907 |
| .22 | .07957 | .23466 | −.07552 | 2.4459 | 3.1221 | 1.7679 |
| .24 | .04465 | .17906 | −.08976 | 2.3251 | 2.9012 | 1.7490 |
| .26 | .01132 | .12783 | −.10519 | 2.2227 | 2.7174 | 1.7280 |
| .28 | −.02076 | .08032 | −.12184 | 2.1349 | 2.5625 | 1.7073 |
| .30 | −.05183 | .03598 | −.13963 | 2.0587 | 2.4307 | 1.6866 |
| .32 | −.08211 | −.00562 | −.15860 | 1.9918 | 2.3177 | 1.6659 |
| .34 | −.11178 | −.04483 | −.17873 | 1.9327 | 2.2201 | 1.6453 |
| .36 | −.14097 | −.08195 | −.19999 | 1.8800 | 2.1353 | 1.6247 |
| .38 | −.16980 | −.11723 | −.22237 | 1.8327 | 2.0611 | 1.6043 |
| .40 | −.19838 | −.15089 | −.24587 | 1.7900 | 1.9960 | 1.5840 |
| .42 | −.22679 | −.18311 | −.27047 | 1.7511 | 1.9385 | 1.5637 |
| .44 | −.25511 | −.21406 | −.29616 | 1.7156 | 1.8876 | 1.5436 |
| .46 | −.28340 | −.24388 | −.32292 | 1.6830 | 1.8424 | 1.5236 |
| .48 | −.31171 | −.27269 | −.35073 | 1.6528 | 1.8020 | 1.5036 |
| .50 | −.34011 | −.30062 | −.37959 | 1.6248 | 1.7658 | 1.4839 |
| .52 | −.36862 | −.32776 | −.40948 | 1.5987 | 1.7332 | 1.4642 |
| .54 | −.39729 | −.35419 | −.44039 | 1.5742 | 1.7038 | 1.4446 |
| .56 | −.42615 | −.38002 | −.47228 | 1.5512 | 1.6772 | 1.4252 |
| .58 | −.45524 | −.40529 | −.50519 | 1.5294 | 1.6530 | 1.4058 |
| .60 | −.48458 | −.43010 | −.53906 | 1.5088 | 1.6310 | 1.3866 |
| .62 | −.51420 | −.45448 | −.57392 | 1.4890 | 1.6107 | 1.3673 |
| .64 | −.54412 | −.47850 | −.60974 | 1.4701 | 1.5921 | 1.3481 |
| .66 | −.57436 | −.50221 | −.64651 | 1.4519 | 1.5748 | 1.3290 |
| .68 | −.60495 | −.52565 | −.68425 | 1.4343 | 1.5588 | 1.3098 |
| .70 | −.63590 | −.54885 | −.72295 | 1.4171 | 1.5439 | 1.2903 |
| .72 | −.66723 | −.57186 | −.76260 | 1.4004 | 1.5299 | 1.2709 |
| .74 | −.69896 | −.59469 | −.80323 | 1.3839 | 1.5168 | 1.2510 |
| .76 | −.73110 | −.61737 | −.84483 | 1.3676 | 1.5044 | 1.2308 |
| .78 | −.76366 | −.63993 | −.88739 | 1.3515 | 1.4926 | 1.2104 |
| .80 | −.79668 | −.66237 | −.93098 | 1.3354 | 1.4815 | 1.1893 |
| .82 | −.83015 | −.68472 | −.97558 | 1.3193 | 1.4708 | 1.1678 |
| .84 | −.86409 | −.70698 | −1.02120 | 1.3030 | 1.4607 | 1.1453 |
| .86 | −.89852 | −.72916 | −1.06788 | 1.2866 | 1.4510 | 1.1222 |
| .88 | −.93346 | −.75126 | −1.11566 | 1.2699 | 1.4417 | 1.0981 |
| .90 | −.96893 | −.77329 | −1.16457 | 1.2528 | 1.4328 | 1.0728 |
| .92 | −1.00493 | −.79526 | −1.21460 | 1.2353 | 1.4242 | 1.0464 |
| .94 | −1.04149 | −.81717 | −1.26581 | 1.2172 | 1.4161 | 1.0183 |
| .96 | −1.07863 | −.83902 | −1.31824 | 1.1985 | 1.4082 | .9888 |
| .98 | −1.11546 | −.86081 | −1.37011 | 1.1792 | 1.4006 | .9578 |
| 1.0 | −1.15280 | −.88253 | −1.42307 | 1.1593 | 1.3932 | .9254 |
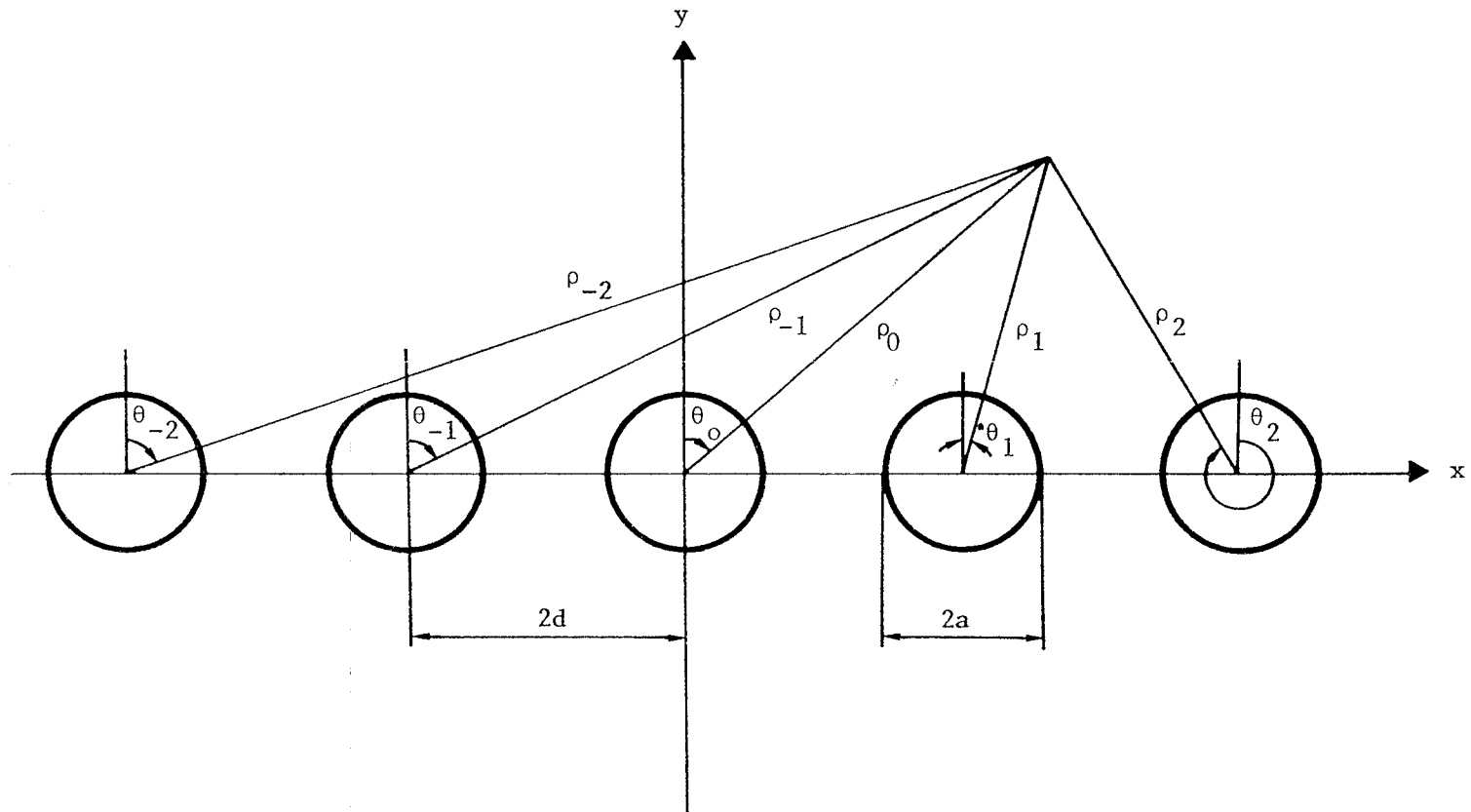
Figure 26. Cross-section of a grid of rods.
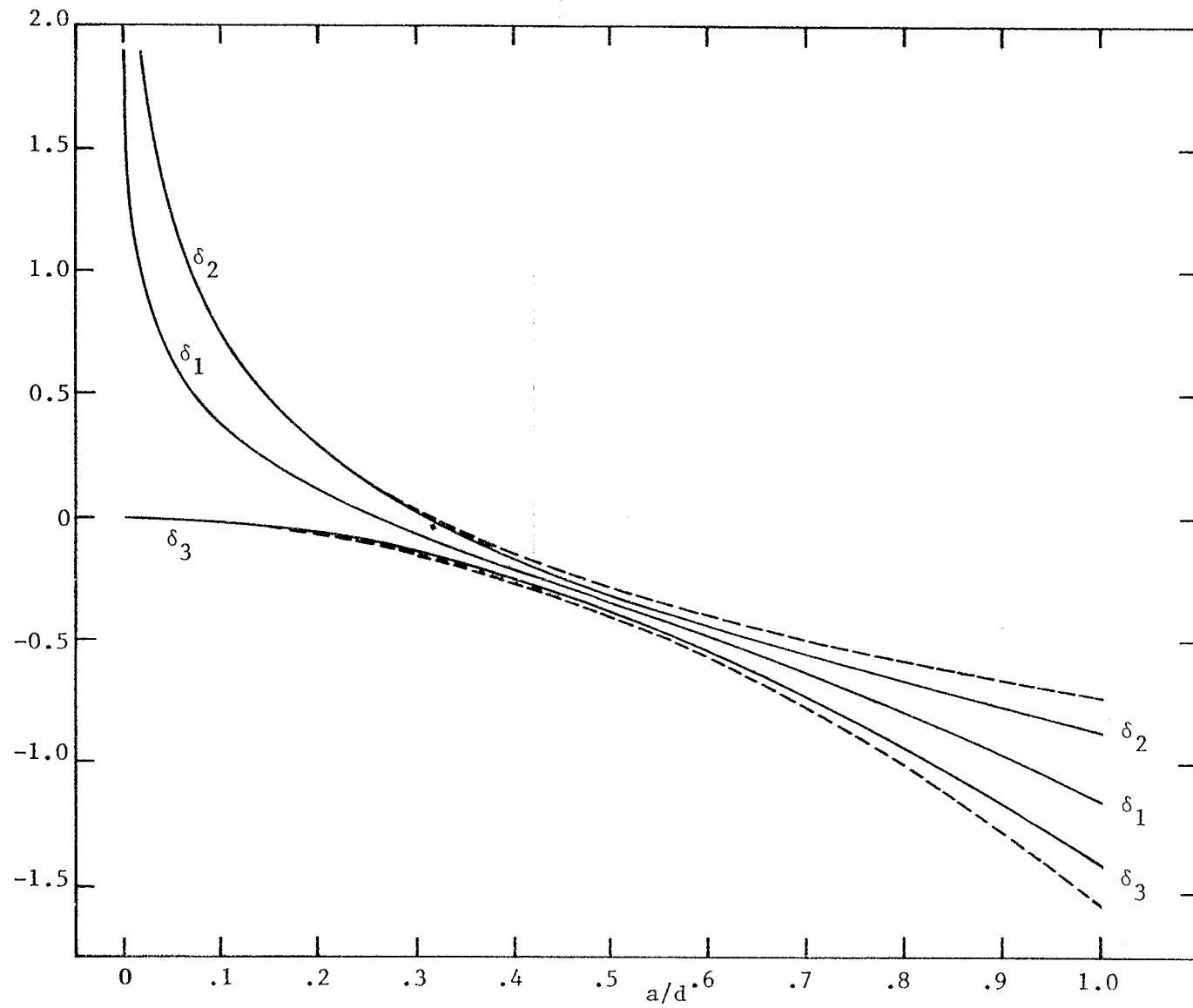
Figure 27. Effective electric position of the grid of rods.
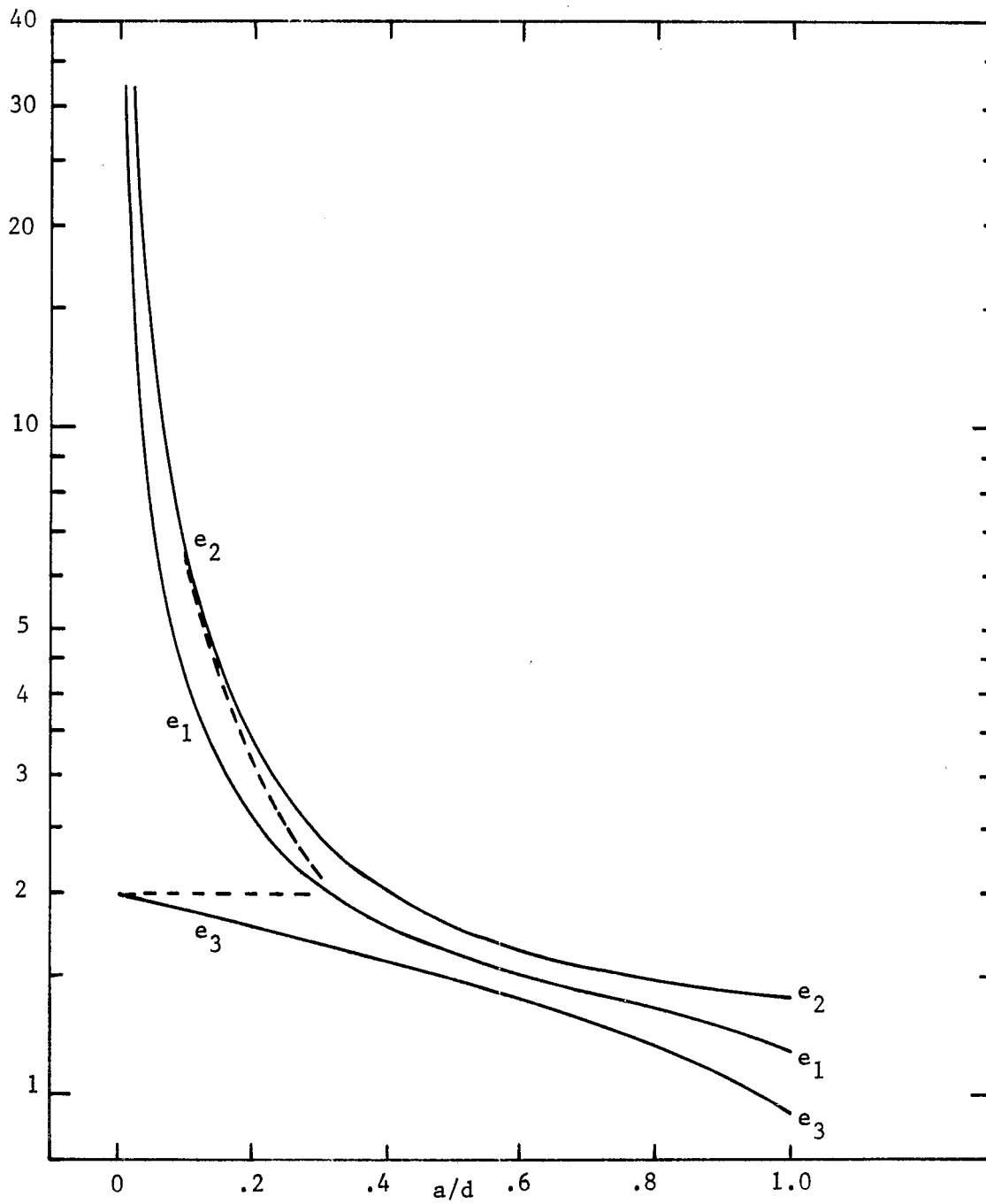
Figure 28. Field enhancement factor of the grid of rods.

## Acknowledgment

## References

1. C. E. Baum, "Impedances and Field Distributions for Parallel Plate Transmission Line Simulators," Sensor and Simulation Note 21, June 1966.

2. R. W. Latham, "Interaction Between a Cylindrical Test Body and a Parallel Plate Simulator," Sensor and Simulation Note 55, May 1968.

3. E. Hallén, Electromagnetic Theory, Chapman and Hall, London, 1962.

4. E. T. Whittaker and G. N. Watson, A Course of Modern Analysis, Cambridge University Press, 1962.

5. M. Abromowitz and I. A. Stegum, Editors, Handbook of Mathematical Functions, National Bureau of Standards, AMS-55, 1964.